Representation of Crystal preferred orientation (CPO)

David Mainprice

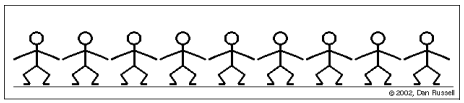

(Géosciences Montpellier, Montpellier, France)

CNRS - Université Montpellier II, 34095 Montpellier, France

Crystal Preferred Orientation (CPO)

- Representation of CPO (PF,IPF,ODF)
- Calculation of CPO (pole figure inversion, 2 theta profile deconvolution, 2D diffraction plate deconvolution)
- Volume Diffraction (x-rays, neutrons)
- Individual orientation measurement (U-stage, EBSD)

Average diffraction properties of radiation used for texture measurement by diffraction, with light also included for comparison

	Light	Neutrons	X-rays	Electrons
Wavelength [nm]	400–700	0.05–0.3	0.05–0.3	0.001–0.01
Energy [eV]	1	10^{-2}	10^{4}	10^{5}
Charge [C]	0	0	0	-1.602×10^{-19}
Rest mass [g]	0	1.67×10^{-24}	0	9.11×10^{-28}
Penetration depth, absorption length [mm]	–	10–100	0.01–0.1	10^{-3}

Texture measurements in rocks

	Polarization microscopy	X-ray goniometry	EBSD
composition	polyphase	monophase	polyphase
crystal symmetry	lower	higher	most
grains size	coarse	fine	wide range
microstructural links	per grain	bulk	submicron resolution
Usage	**demanding**	**selective**	**expanding**

Kunze (2005)

Overview of the Most Common Techniques for Determination of Local Orientations

Method	Technique	Spatial Resolution[a]	Angular Accuracy	Application
TEM	CBED	1 nm	0.1°	Polycrystals (grains, subgrains, deformed microstructure, inhomogeneities, recrystallization nuclei, …)
	MBED	10 nm	0.2°	
	SAD	1 μm	5°	
SEM	EBSD	<0.1 μm	0.5°	Polycrystals (grains, subgrains)
	SAC	10 μm	0.5°	Polycrystals (grains)
	Micro-Kossel	10 μm	0.5°	Polycrystals (grains)
X-ray diffraction	Conventional Laue	100 μm	2°	Single crystals, very coarse grains
	Synchrotron based	0.1–100 μm	0.1°	Polycrystals (grains)
Optical techniques	Selective ({111}) etching	1 μm	5°–10°	Polycrystals (grains)
	Etch pits	20–100 μm	>10°	Polycrystals (coarse grains)

[a]Diameter of the minimum detectable sample area.

Over view

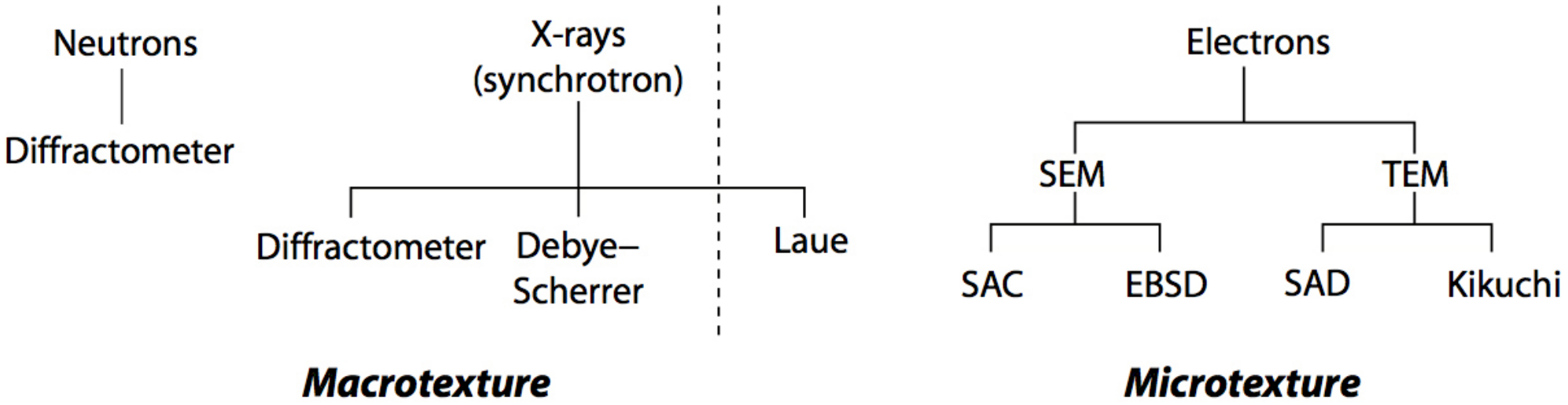

Categorization of the mainstream techniques for texture determination according to the radiation used as a probe. Macrotexture and microtexture methods are on the left- and right-hand parts of the diagram, respectively.

Representation of CPO

- Pole figure
- Inverse Pole figue
- Orientation distribution function ...

Representation on a projection

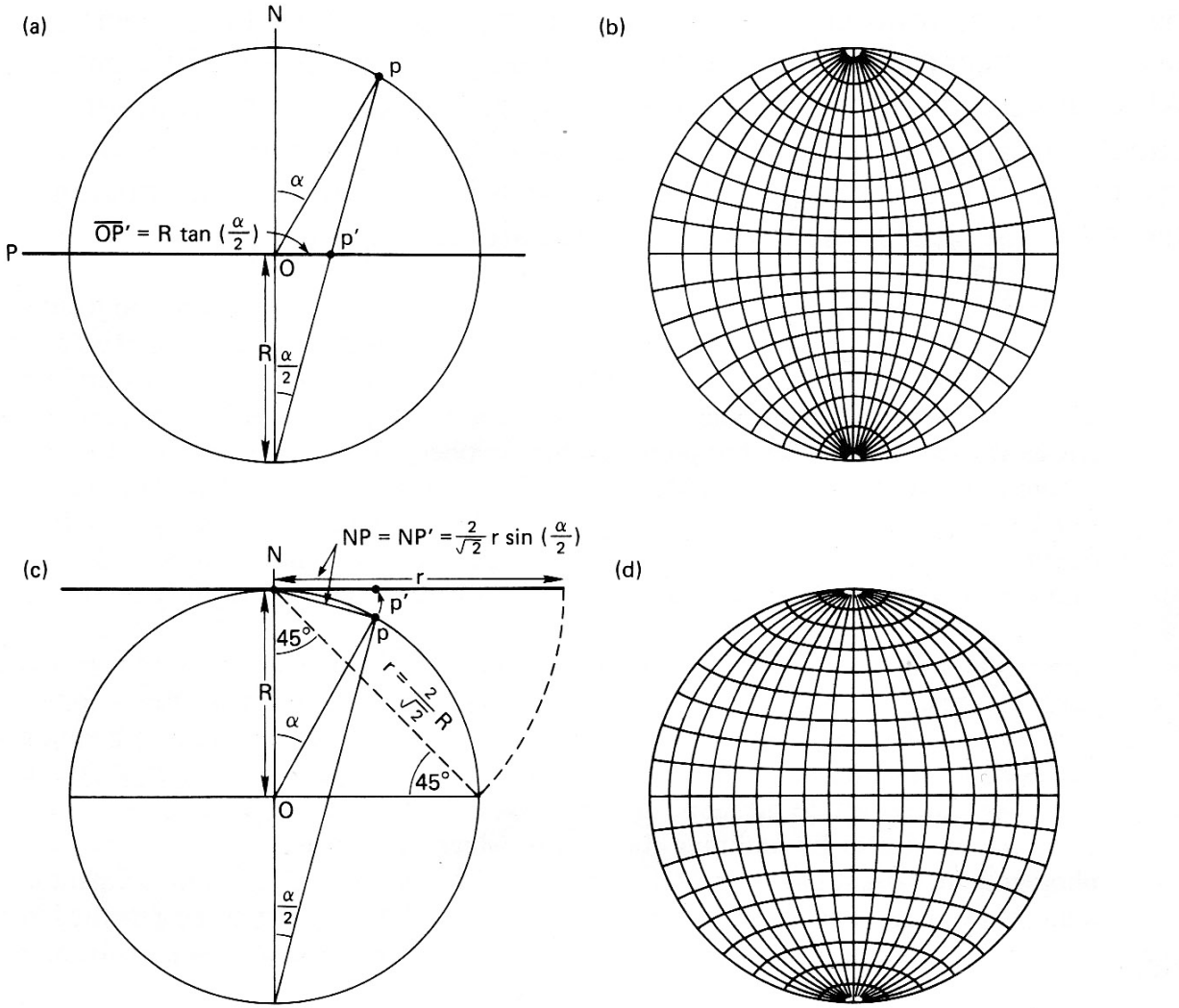

Stereographic (a, b) and equal-area (c, d) projection. (a, c) illustrate the principle of projection; (b, d) are projections of a 10° × 10° coordinate grid on the sphere.

Equal angle or Equal area

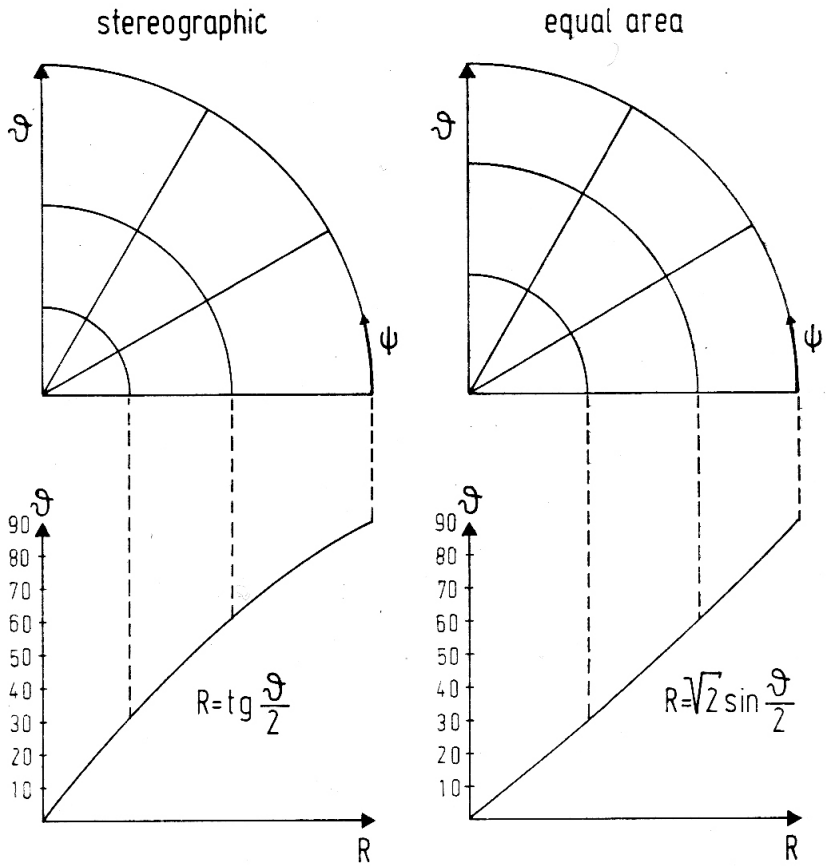

Figure 2.27 The stereographic and the equal area projections. The scale of the angle ϑ is given by $\tan\frac{\vartheta}{2}$ *and* $\sqrt{2}\,\sin\frac{\vartheta}{2}$, *respectively*

For CPO work use Equal area

5000 Random orientations

Equal angle pole figure

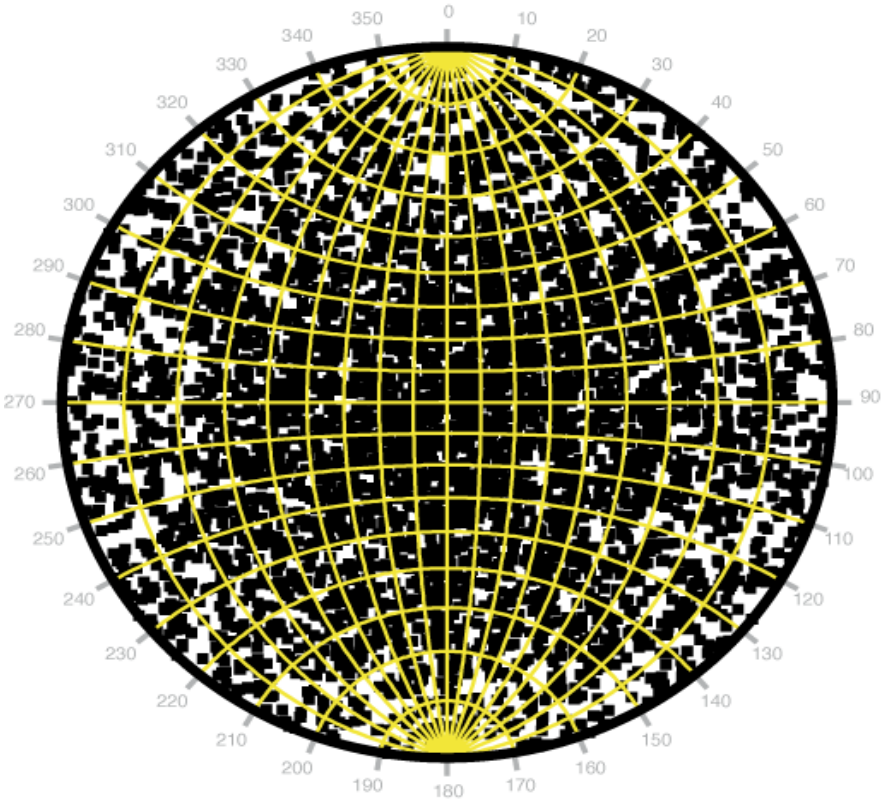

Equal area pole figure

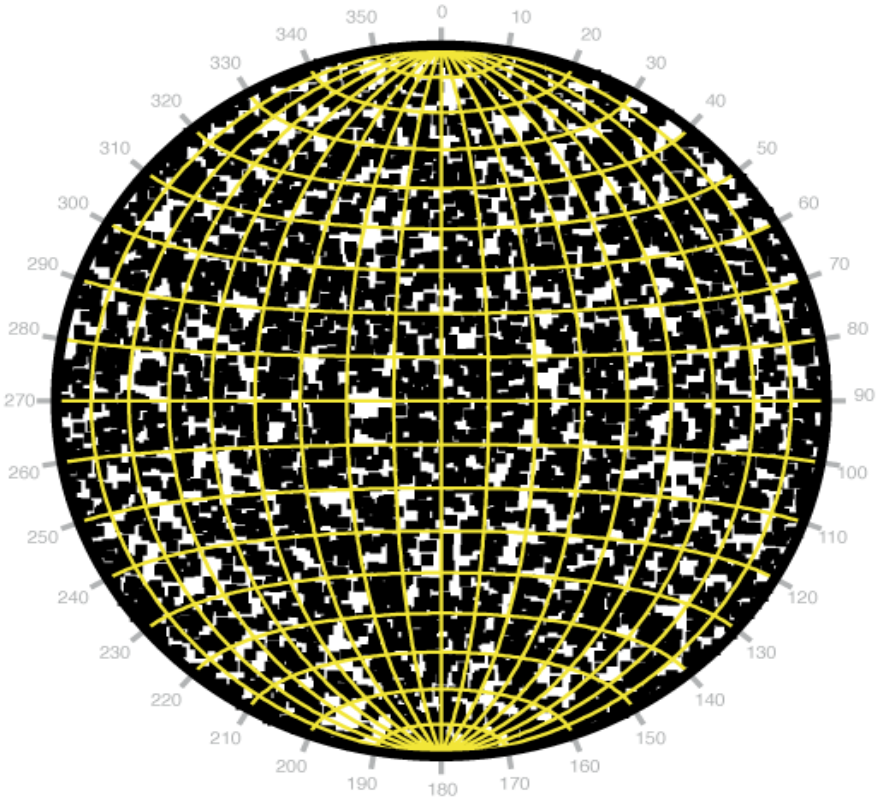

Define an orientation ?

- Euler angles
- Rotation axis and angle
- Orientation matrix

Three Euler angles – 3 rotations

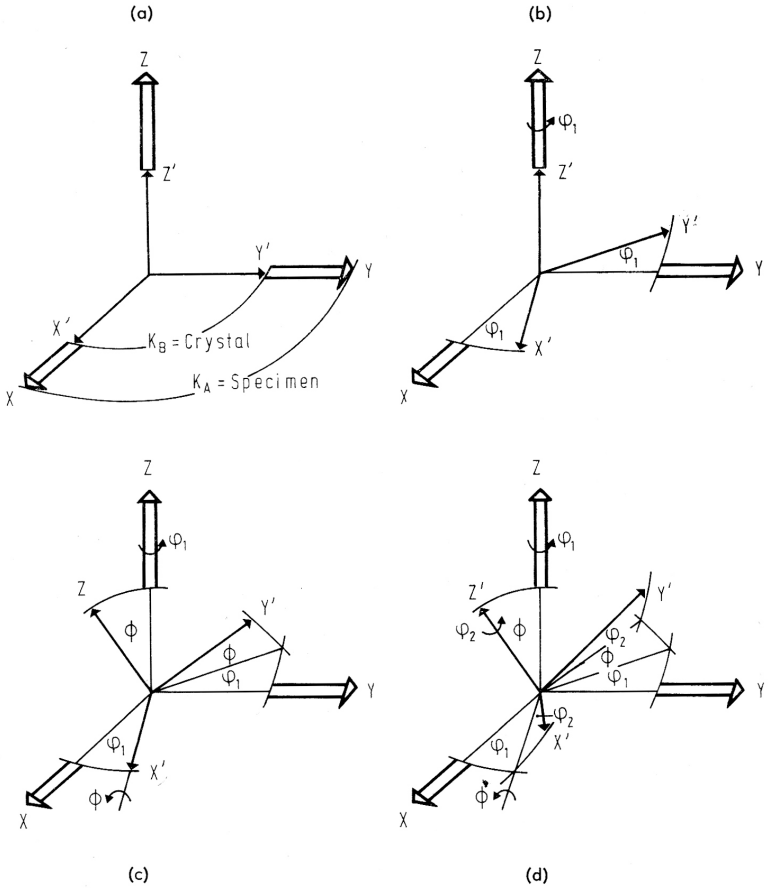

Figure 2.2 On the definition of the EULER *angles $\varphi_1\Phi\varphi_2$: (a) the crystal coordinate system $K_B(X'Y'Z')$ lies parallel to the sample coordinate system $K_A(XYZ)$ (so-called cube orientation); (b) the crystal coordinate system is rotated about the Z'-axis through the angle φ_1; (c) the crystal coordinate system K_B is rotated with respect to the orientation (b) around the X'-axis through the angle Φ; (d) the crystal coordinate system K_B is rotated with respect to the orientation (c) around the Z'-axis through the angle φ_2*

Euler Angles – Bunge convention

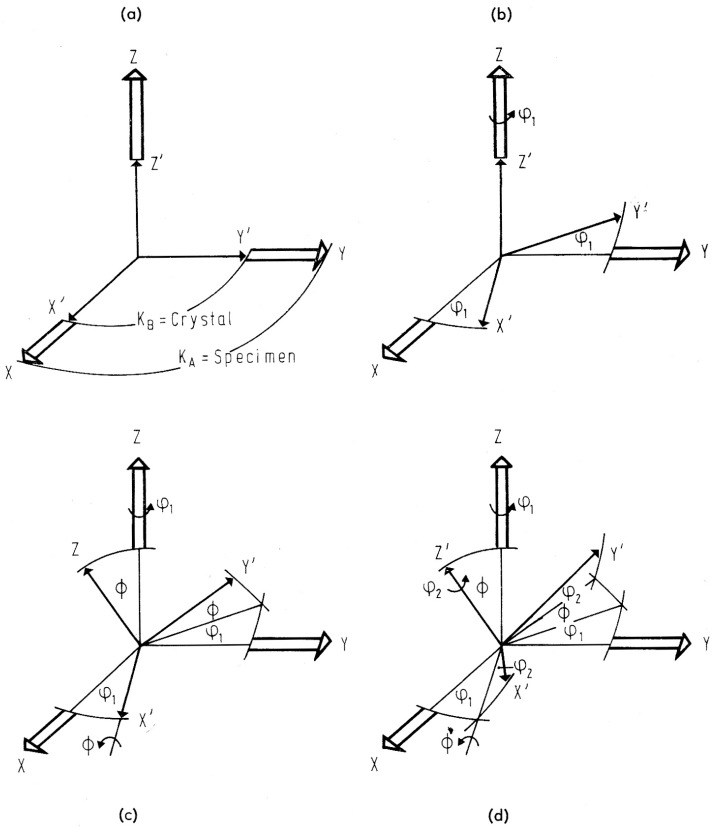

Figure 2.2 On the definition of the EULER *angles $\varphi_1 \Phi \varphi_2$: (a) the crystal coordinate system $K_B(X'Y'Z')$ lies parallel to the sample coordinate system $K_A(XYZ)$ (so-called cube orientation); (b) the crystal coordinate system is rotated about the Z'-axis through the angle φ_1; (c) the crystal coordinate system K_B is rotated with respect to the orientation (b) around the X'-axis through the angle Φ; (d) the crystal coordinate system K_B is rotated with respect to the orientation (c) around the Z'-axis through the angle φ_2*

Bunge Euler Angles

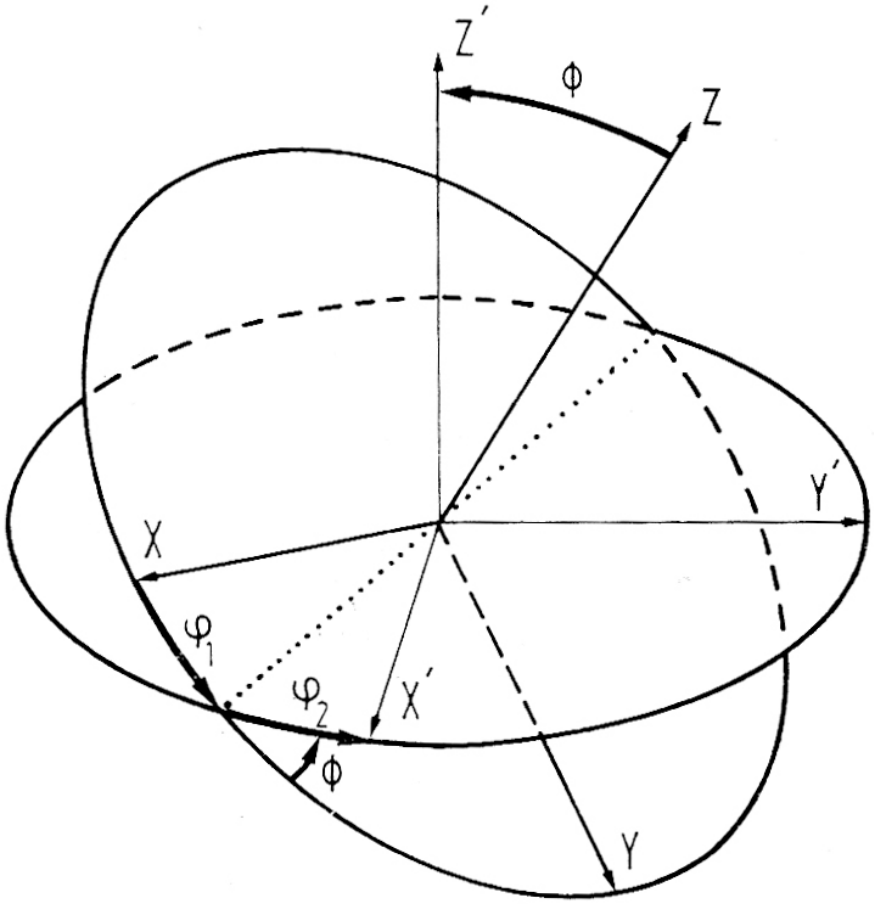

Figure 2.3 On the definition of the EULER *angles* $\varphi_1 \Phi \varphi_2$

Cartesian Reference Frame I

- Measurement of orientation using Euler angles requires the definition of a right-handed Cartesian (also called orthonormal) system in crystal co-ordinates.
- For cubic, tetragonal and orthorhombic the obvious choice is to use the orthogonal lattice basis vectors **a**[100], **b**[010] and **c**[001] of the crystal axes. However, for most general case of triclinic crystal symmetry where **a**, **b**, and **c** are not orthogonal, there are many possible choices and no general convention.
- The choice of a specific reference frame is often imposed by the EBSD software, but users are often not aware what choice has been made.

Cartesian Reference Frame II

- Here are 3 possible choices, for the tensor Cartesian reference frame for Euler angles ($\mathbf{e_1}$,$\mathbf{e_2}$,$\mathbf{e_3}$) ;
- a) $\mathbf{e_3}$ = **c**[001], $\mathbf{e_2}$= **b*** ⊥(010) and hence for a right-handed system $\mathbf{e_1}$ = $\mathbf{e_2}$ **x** $\mathbf{e_3}$ (e.g. BearTex software)
- b) $\mathbf{e_3}$ = **c**[001] , $\mathbf{e_1}$= **a*** ⊥(100) and $\mathbf{e_2}$ = $\mathbf{e_3}$ **x** $\mathbf{e_1}$ (e.g. HKL Channel software)
- c) $\mathbf{e_3}$ = **c***⊥ (001) , $\mathbf{e_1}$= **a**[100] and $\mathbf{e_2}$ = $\mathbf{e_3}$ **x** $\mathbf{e_1}$

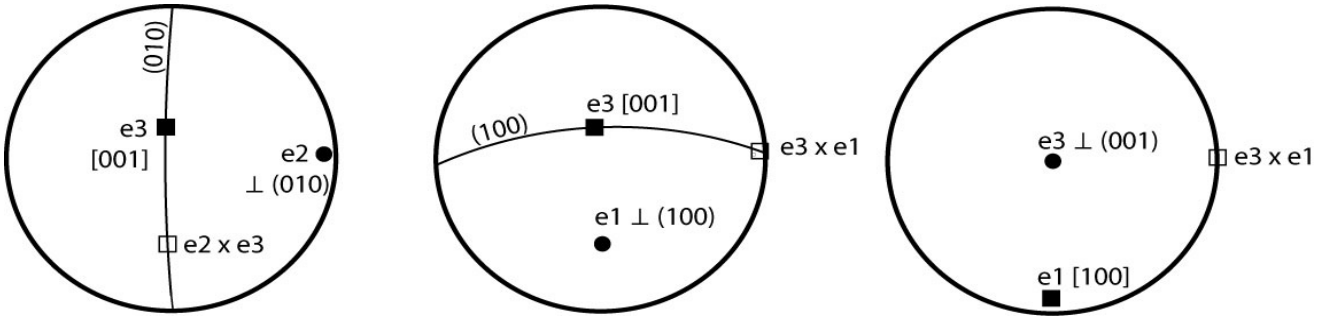

Reference Frames a), b) and c) for triclinic plagioclase Labradorite An66 (**a**=0.817 nm **b**=1.287 nm **c**=1.420 nm α=93.46° β=116.09° γ=90.51°)

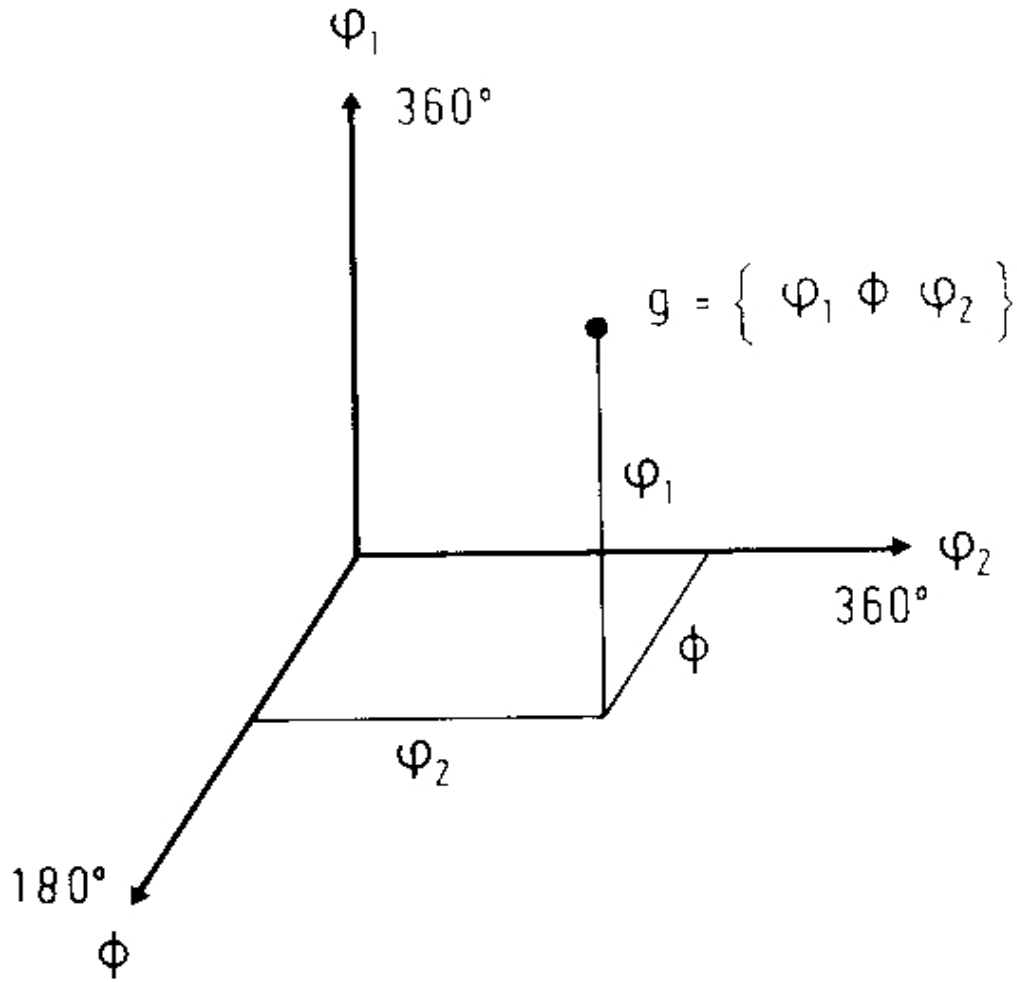
φ1
360°
g = { φ1 Φ φ2 }
φ1
φ2
360°
Φ
φ2
180°
Φ

ODF – Unit and asymmetric unit

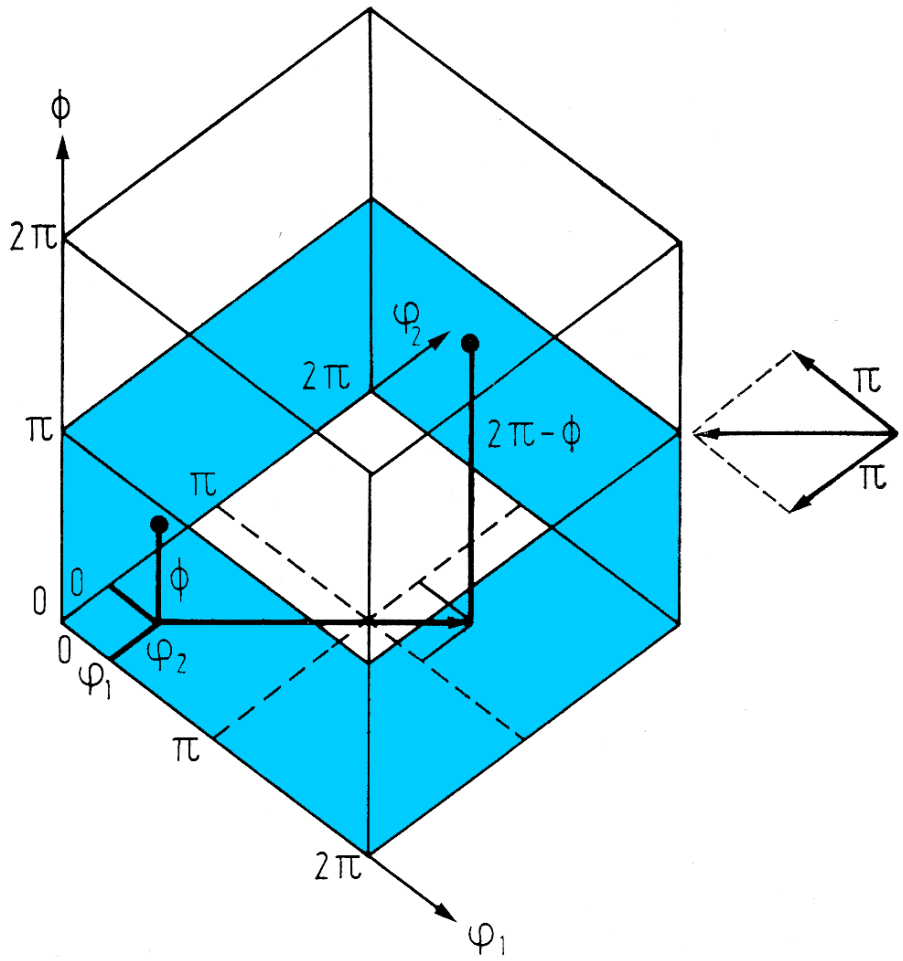

Unit cell and asymmetric unit in EULER *space*

Euler Space : Asymmetric Unit

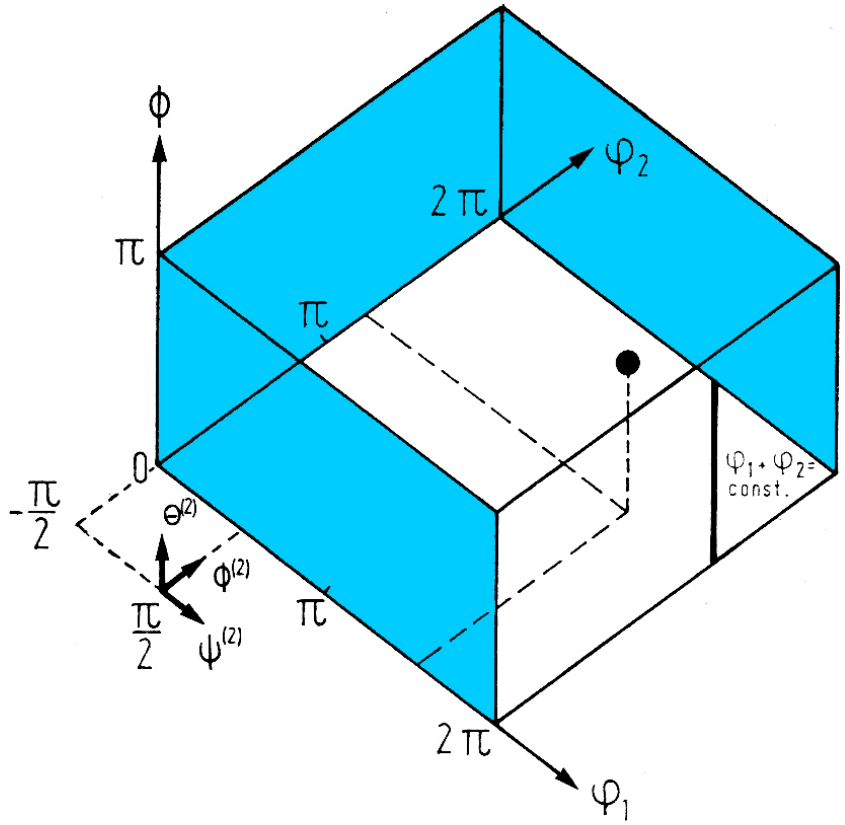

The orientation space (EULER *space*) *corresponding to the two definitions of the* EULER *angles* $\varphi_1 \Phi \varphi_2$ *and* $\Psi\ \Theta\ \Phi$. *Points on the lines* $\Phi = 0$, $\varphi_1 + \varphi_2 = \text{const.}$ *represent the same rotation or orientation*

ODF

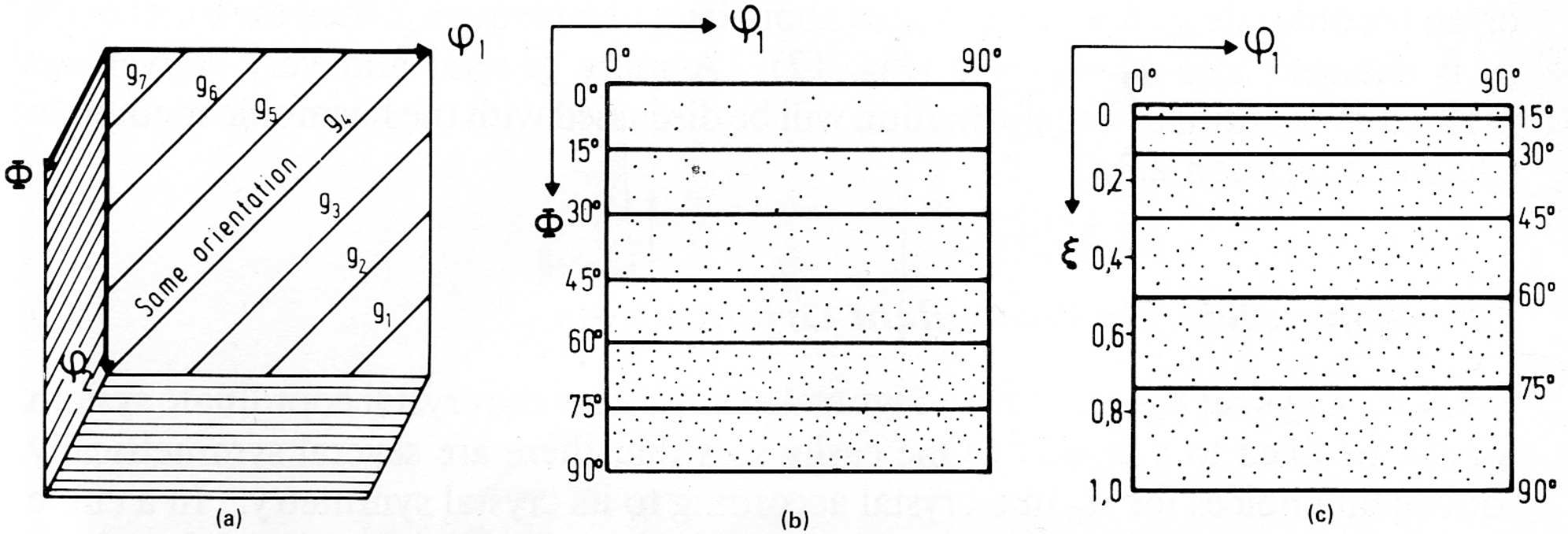

Fig. 11 (a) The structure of the plane $\Phi = 0$ in the Euler space. (b) The metric in the Euler space $\varphi_1 \Phi \varphi_2$. (c) The metric in the space $\varphi_1 \xi \varphi_2$.

ODF of 10 000 random orientations

Projection ϕ_2

	ϕ_1	Φ	ϕ_2
Orthorhombic crystal symmetry and triclinic sample symmetry :	0-180°	0-180°	0-180°

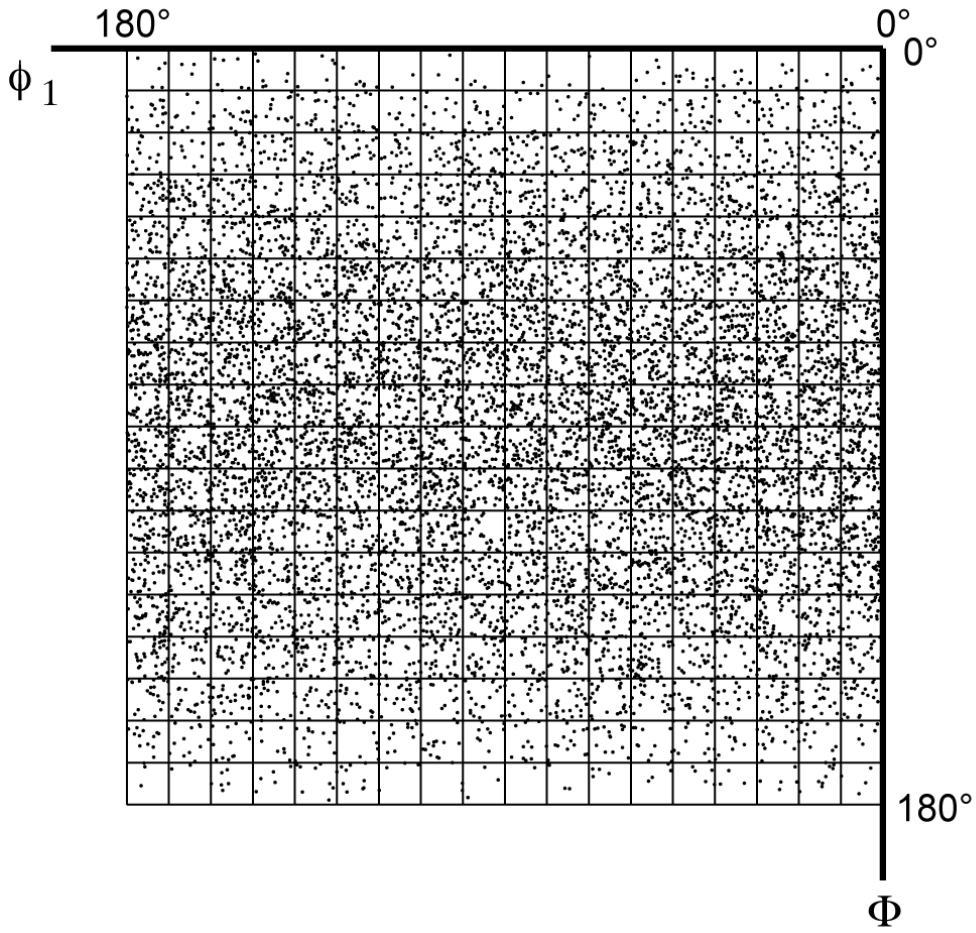

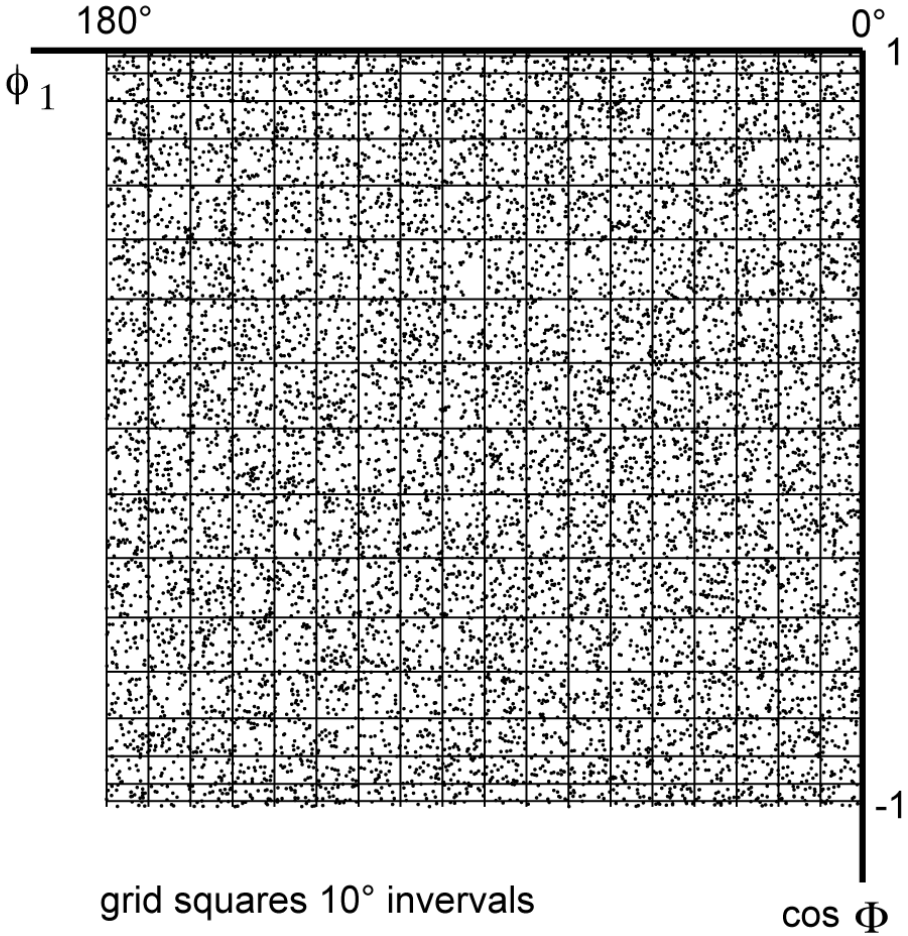

grid squares 10° invervals

Orientation distribution

Orientations

$g_n = (\varphi_1, \Phi, \varphi_2)_n$

(n = 1…N)

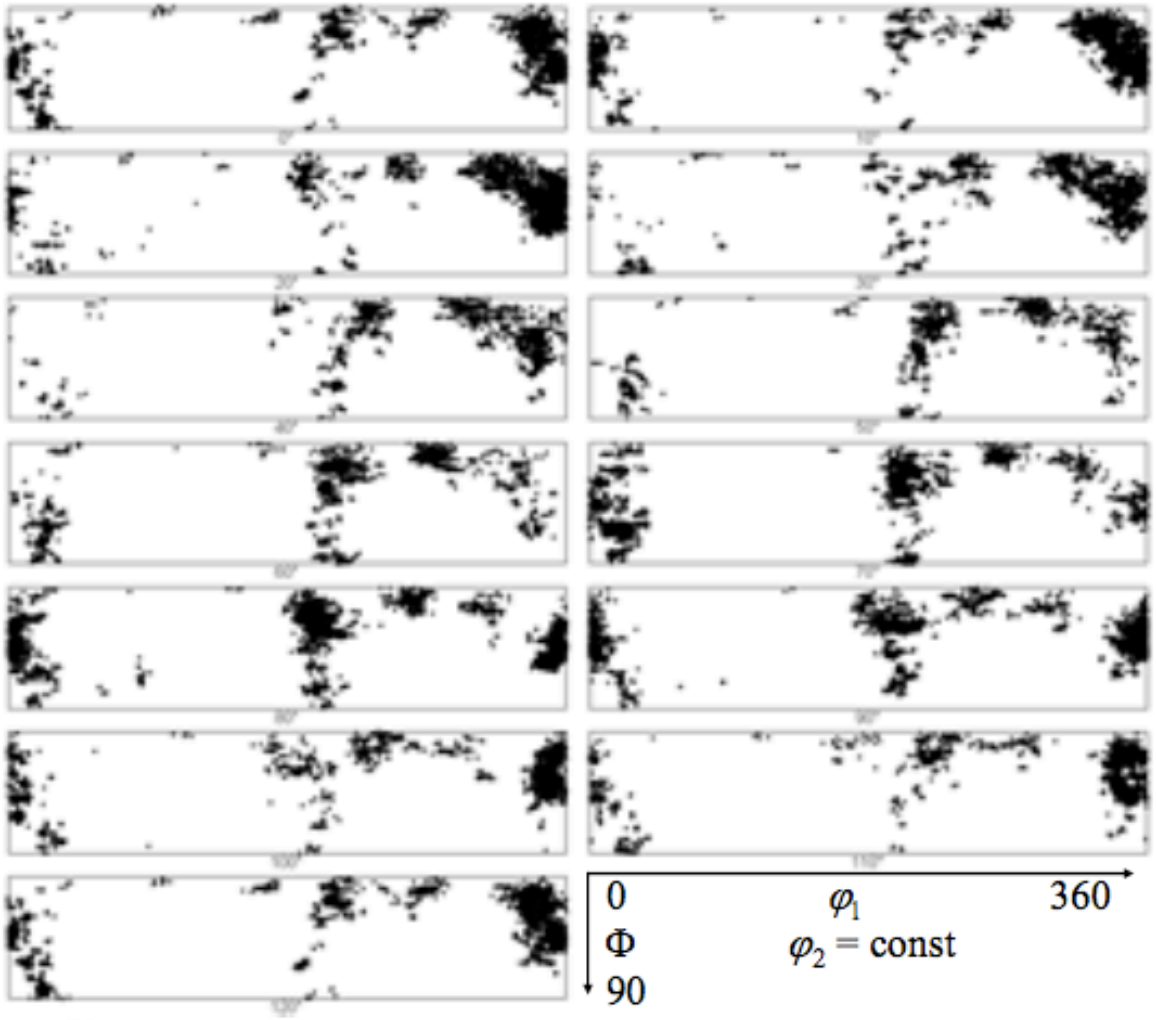

Recrystallized quartzite,
Bergell Alps

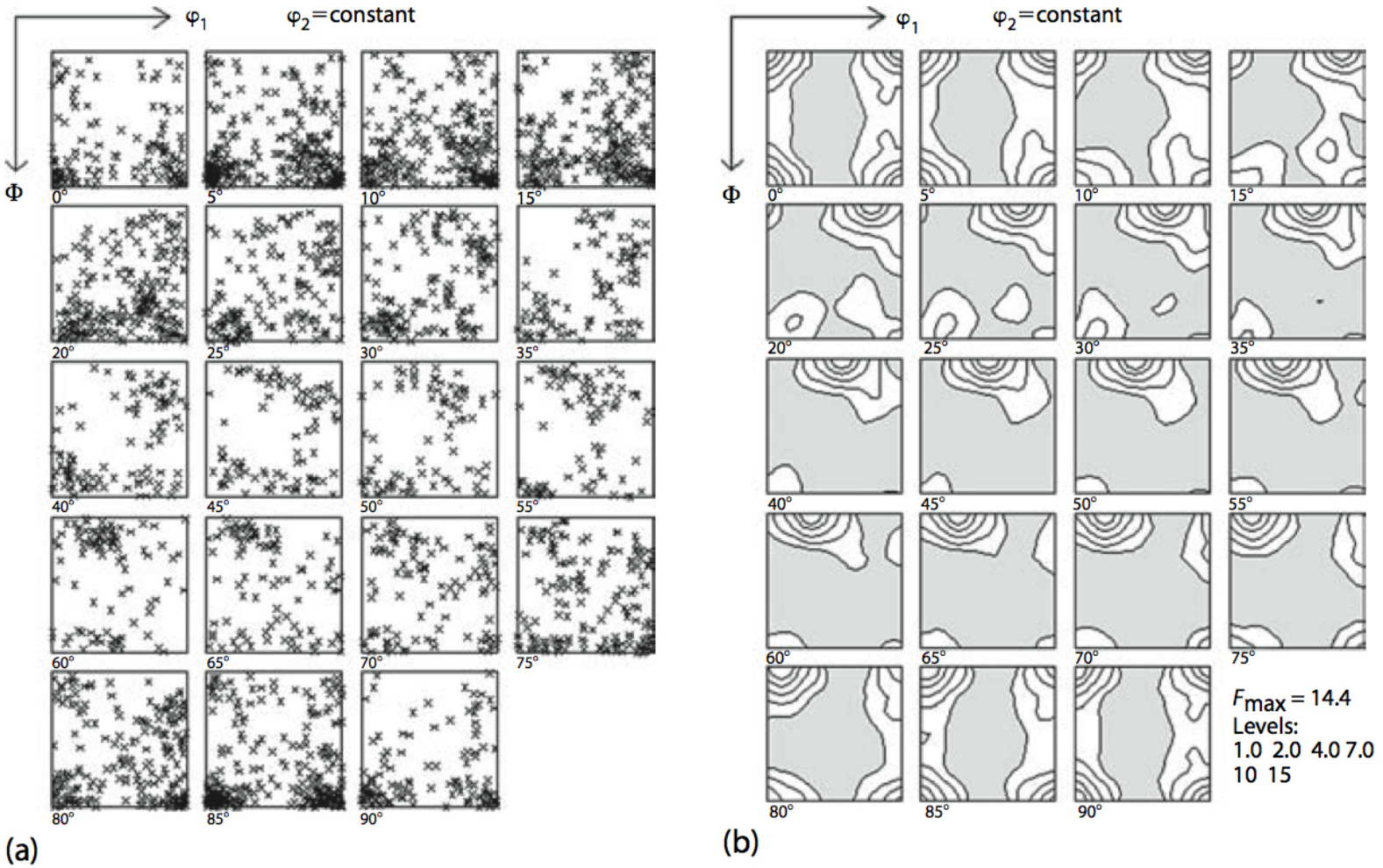

Presentation in Euler space of microtexture data of a recrystallized aluminum sample. (a) Orientations of 1000 grains as obtained by EBSD; (b) continuous intensity function (ODF) as derived from x-ray pole figure measurements of the same sample, showing good reproducibility of the main texture features.

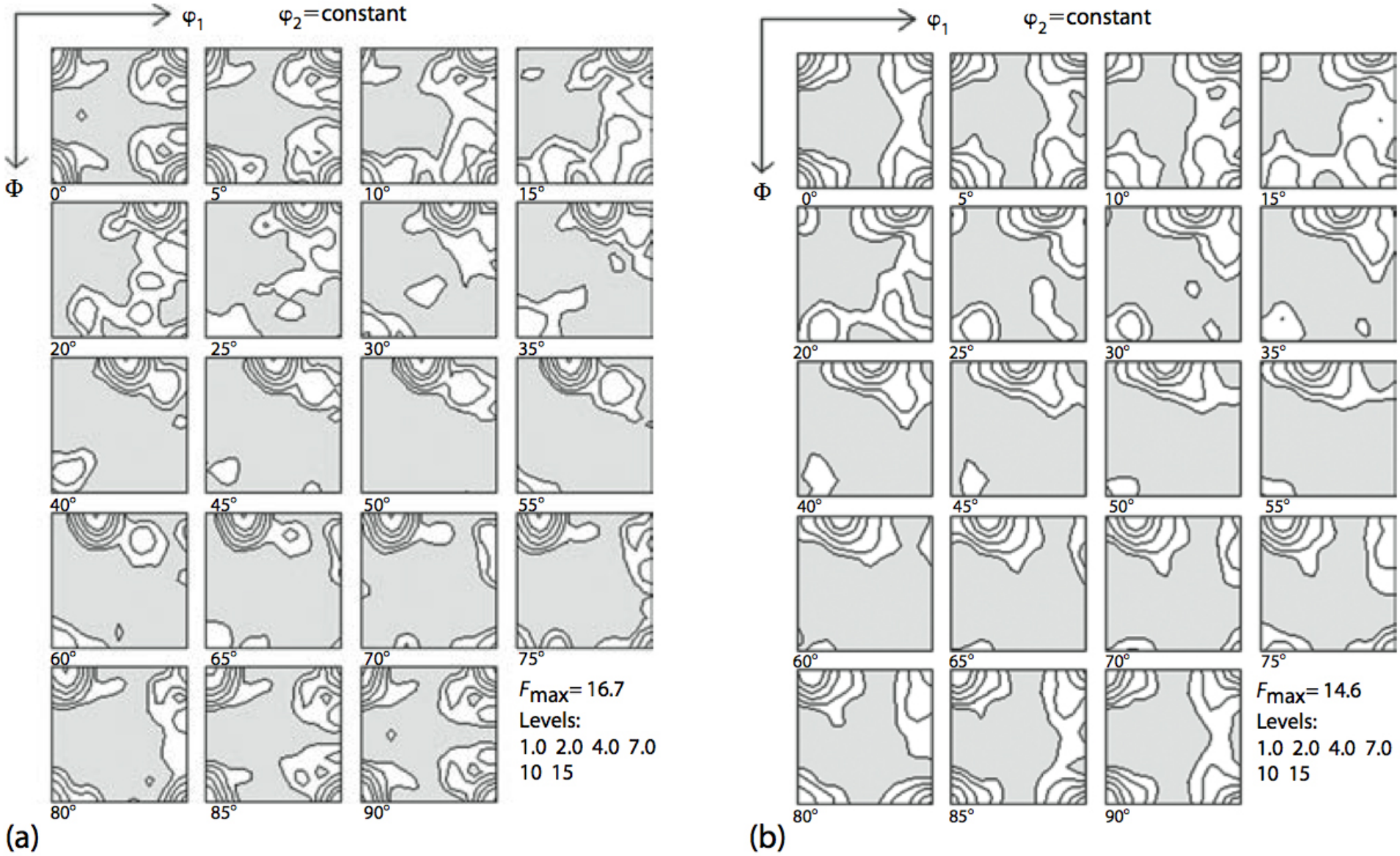

ODFs of recrystallized aluminum, as in Figure 9.5, calculated from different numbers N of EBSD single-grain orientation measurements, (a) $N = 100$, (b) $N = 1000$.

Orientation Distribution Function

The orientation distribution function (O.D.F.) f(**g**) is defined as the volume fraction of orientations with an orientation in the interval between **g** and **g**+d**g** in a space containing all possible orientations given by

$$\Delta V/V = \int f(\mathbf{g})\, d\mathbf{g}$$

where $\Delta V/V$ is the volume fraction of crystals with orientation **g**, f(**g**) is the texture function and $d\mathbf{g} = 1/8\pi^2 \sin\phi\, d\varphi 1 d\phi\, d\varphi 2$ is the volume of the region of integration in orientation space.

The function f(**g**) is given in terms of symmetrical generalized spherical harmonics (Bunge,1982) as

$$f(\mathbf{g}) = \sum_{l=0}^{Lmax} \sum_{m=l}^{M(l)} \sum_{n=-l}^{l} C_l^{mn}\, T_l^{mn}(\mathbf{g})$$

C_l^{mn} are the coefficients of the series development of the texture function f(**g**), $T_l^{mn}(\mathbf{g})$ are the generalised spherical harmonic functions, M(l) is the number of linearly independent harmonics and Lmax is the maximum degree used in the expansion. For tensor properties of rank 2 or 4 the maximum degree of expansion is Lmax=2 or Lmax=4 repectively.

Pole figure comparison : FB085 Olivine100 grains (U-stage)

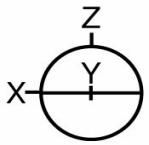

(100) (010) (001)

PF2k
(box counting with
gaussian half-width = 8.5°)

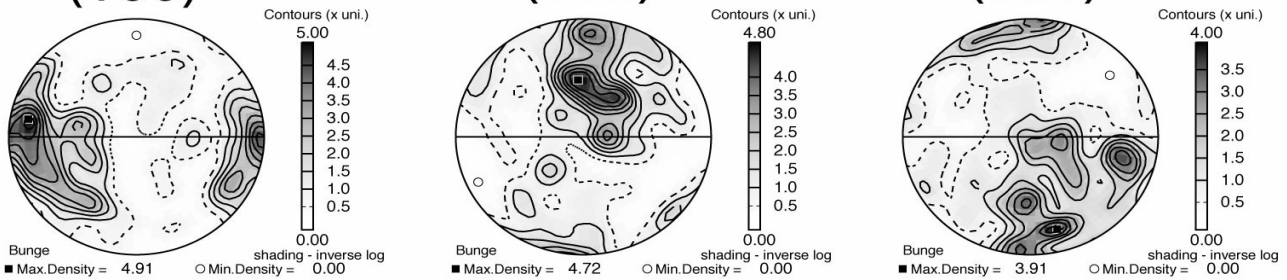

CGRAIN
(SH Even Coeffs Lmax=22
by F.Wagner Metz
gaussian half-width =10°)

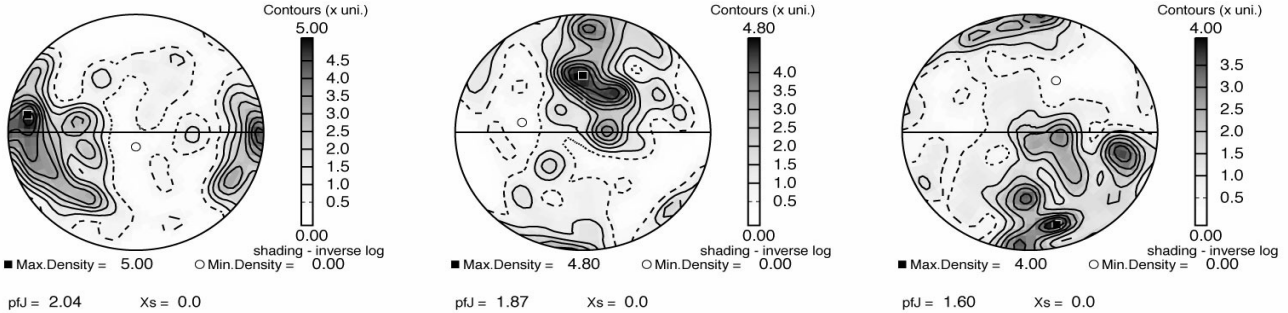

CGRAIN
(SH Even Coeffs Lmax=4
by F.Wagner Metz
gaussian half-width =10°)

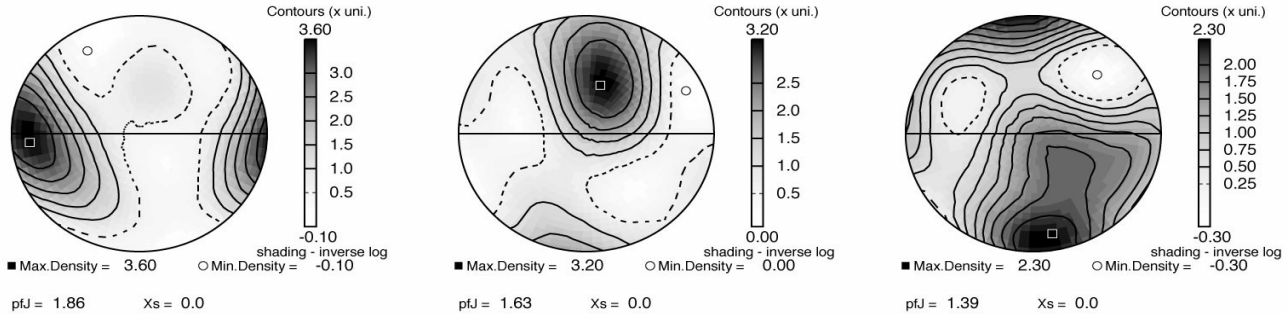

CGRAIN
(SH Even Coeffs Lmax=2
by F.Wagner Metz
gaussian half-width =10°)

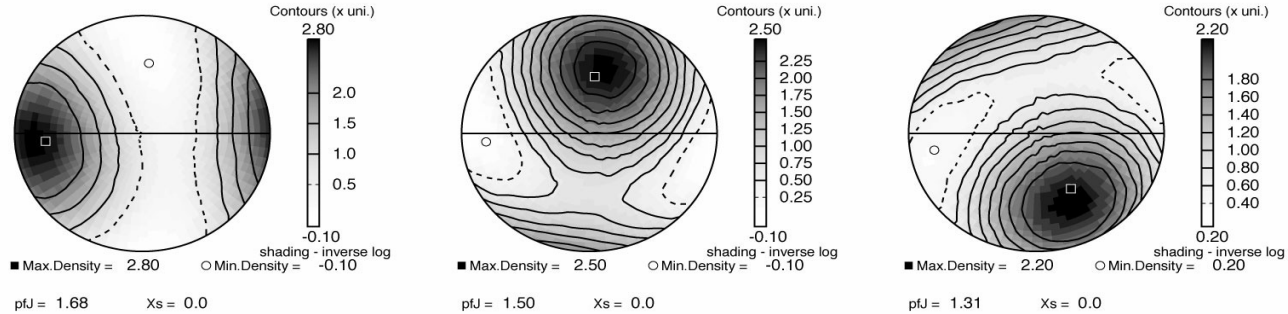

Elastic properties of aggregate

The elastic properties of the polycrystal may be calculated by integration over all possible orientations of the ODF. Bunge (1985) has shown that integration is given as:

$$\langle C_{ijkl} \rangle^m = \int C_{ijkl}^m(\mathbf{g}).f(\mathbf{g})\, dg$$

where $\langle C_{ijkl} \rangle^m$ is the elastic properties of the aggregate of mineral m.

Alternatively it may be determined by simple summation of individual orientation measurements (e.g. U-stage or EBSD),

$$\langle C_{ijkl} \rangle^m = \sum C_{ijkl}^m(\mathbf{g}).v(\mathbf{g})$$

where $v(\mathbf{g})$ is the volume fraction of the grain in orientation **g.**

Orientation Distribution Function & J index

Measured ODF : f(g) - series of individual orientations g1,g2,g3...gn

$g = \{\varphi 1\ \phi\ \varphi 2\}$ $dV/V = f(g)\, dg$ $\int f(g)\ dg = 1$ $dg = d\varphi 1\ d\phi\ d\varphi 2 \sin\phi / 8\pi^2$

$$J = \int f(g)^2 dg$$

1-D Representation

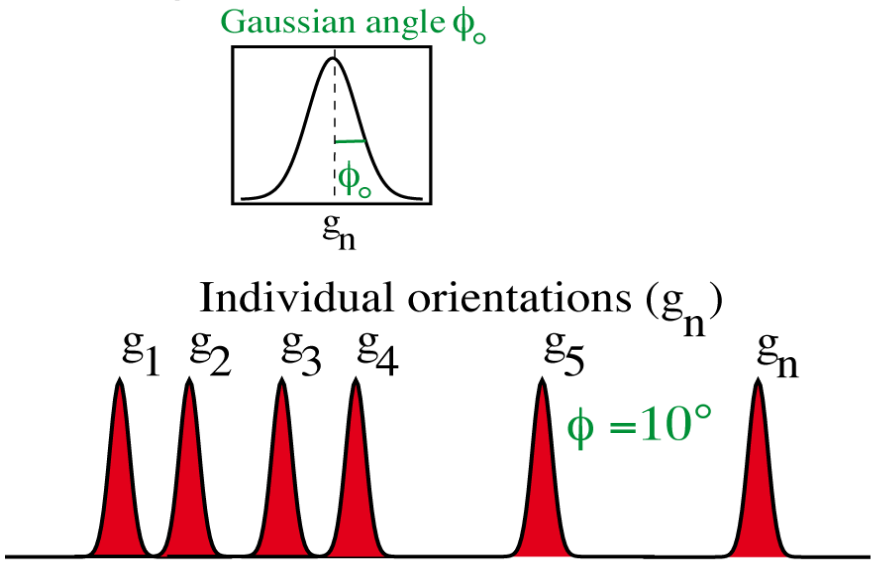

3-D Representation

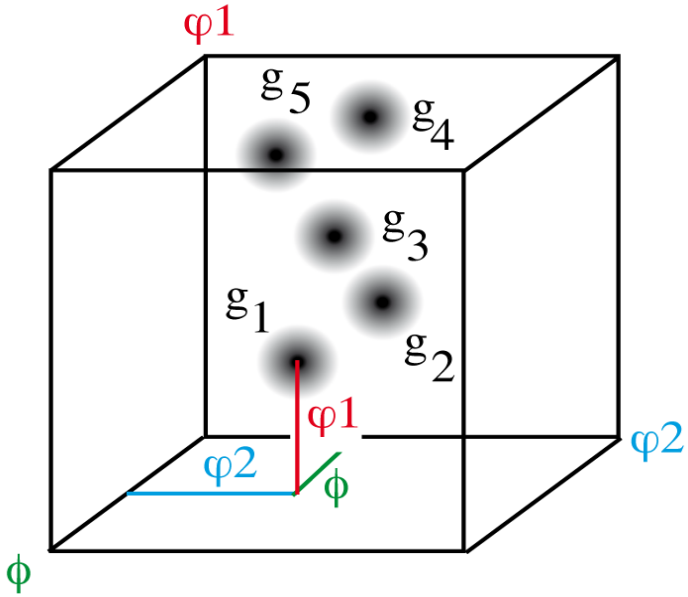

Rotation axis and angle

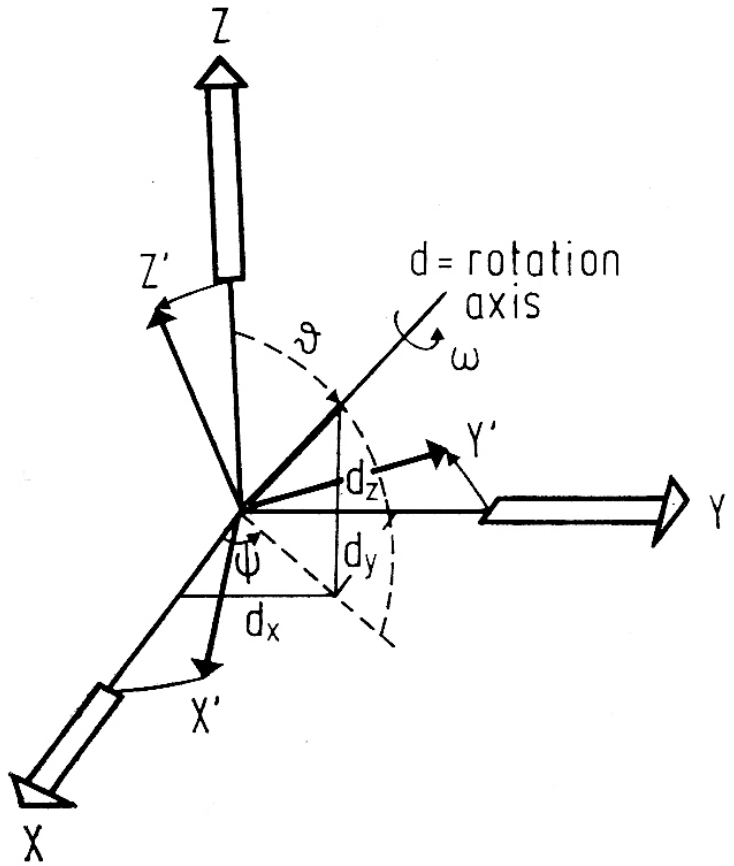

Figure 2.8 Representation of a rotation by the rotation axis $\mathbf{d}$ *and the appropriate rotation angle* ω*. The rotation axis is described either by its direction cosines* $d_x\ d_y\ d_z$ *or by polar coordinates* $\vartheta\varphi$

Orientation g

Orientation of crystals in a polycrystal can be measured by volume diffraction techniques (e.g. X-ray or neutron diffraction) or individual orientation measurements (e.g. U-stage & Optical microscope, electron channeling or EBSD).

An orientation, often given the letter **g**, of a grain or crystal in sample co-ordinates can be described by the rotation matrix between crystal and sample co-ordinates. In practice it is convenient to describe the rotation by a triplet of Euler angles, for example $\mathbf{g} = \varphi 1 \phi \varphi 2$ used by Bunge (1982).

N.B. One should be aware there are many different definitions of Euler angles (at least 10 !) that are used in the physical sciences, here we will use the definition given by Bunge (1982).

Orientation of a crystal defined by 3 Euler angles

XYZ - Specimen Frame

X'Y'Z' - Crystal Frame

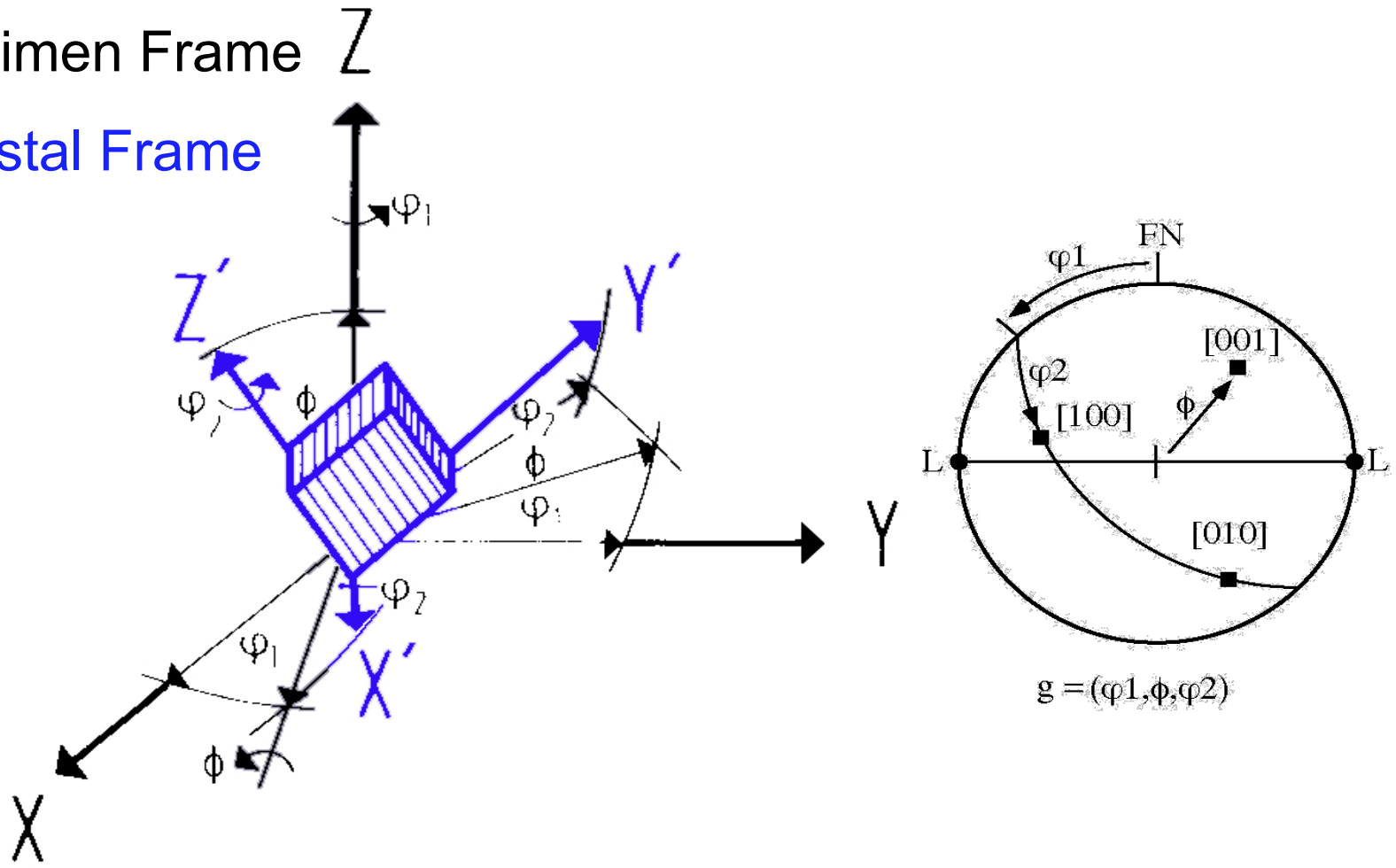

Beware there many different conventions - here the convention of Bunge (1982)

Euler Angles

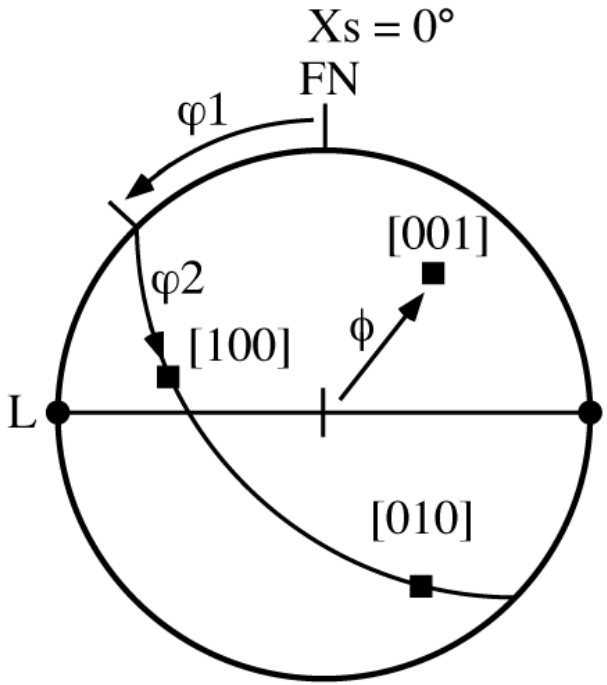

Xs = 0° azimuth

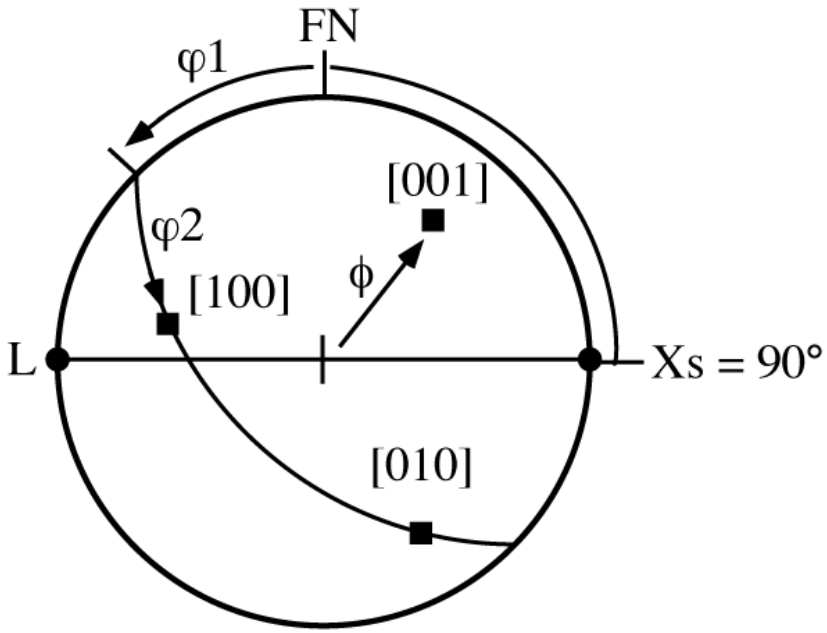

Xs = 90° azimuth

Pole figure : crystallographic directions in sample reference x,y,z axes

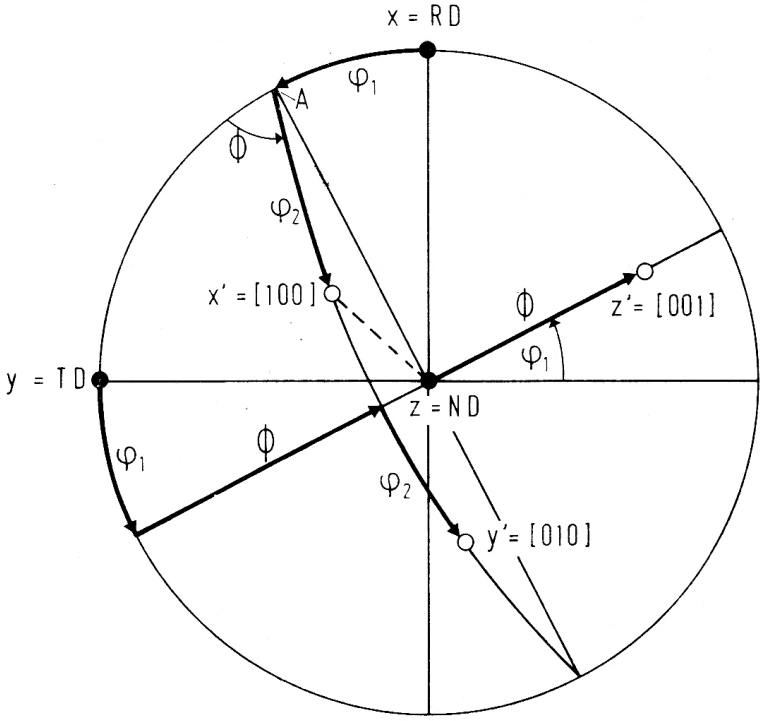

Figure 2.22 The orientation of the crystal directions $X' = [100]$, $Y' = [010]$ $Z' = [001]$ *in the stereographic projection in the sample coordinate system (pole figure) expressed by the* EULER *angles* $\varphi_1 \Phi \varphi_2$

Example of a single crystal

Non-polar and Polar properties

Non-polar case:

centro-symmetric
symmetry
property the same value
in +ve and -ve direction

Example elasticity

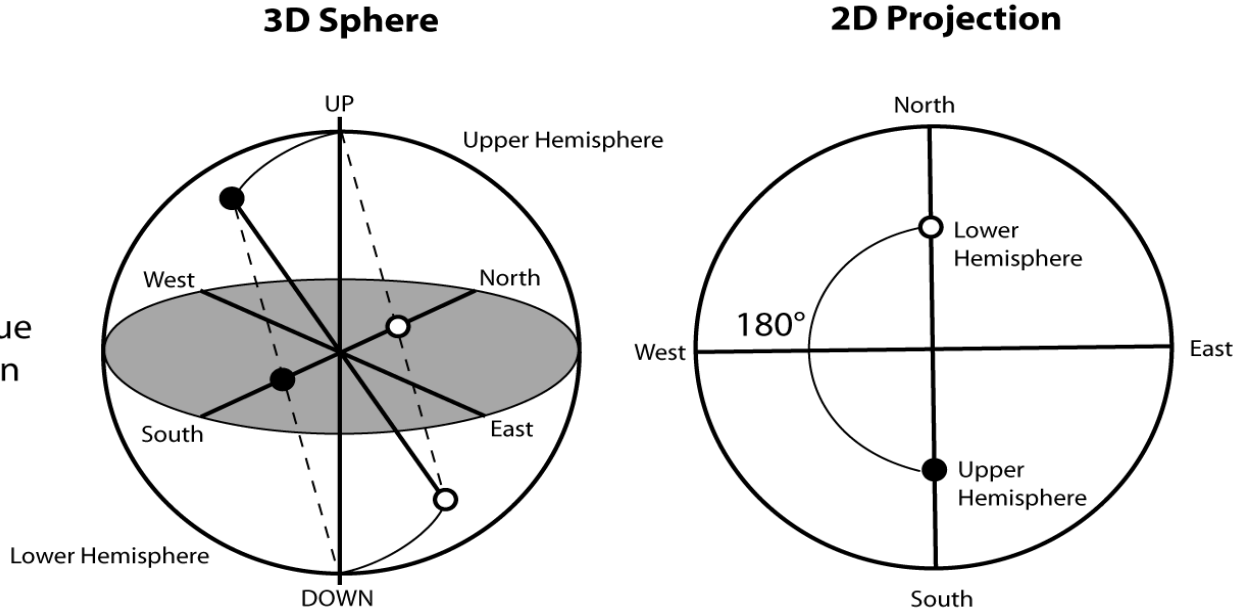

Polar case:

no centre of symmetry
property has different values
in +ve and -ve direction

Example piezoelectricity
in quartz along a-axes

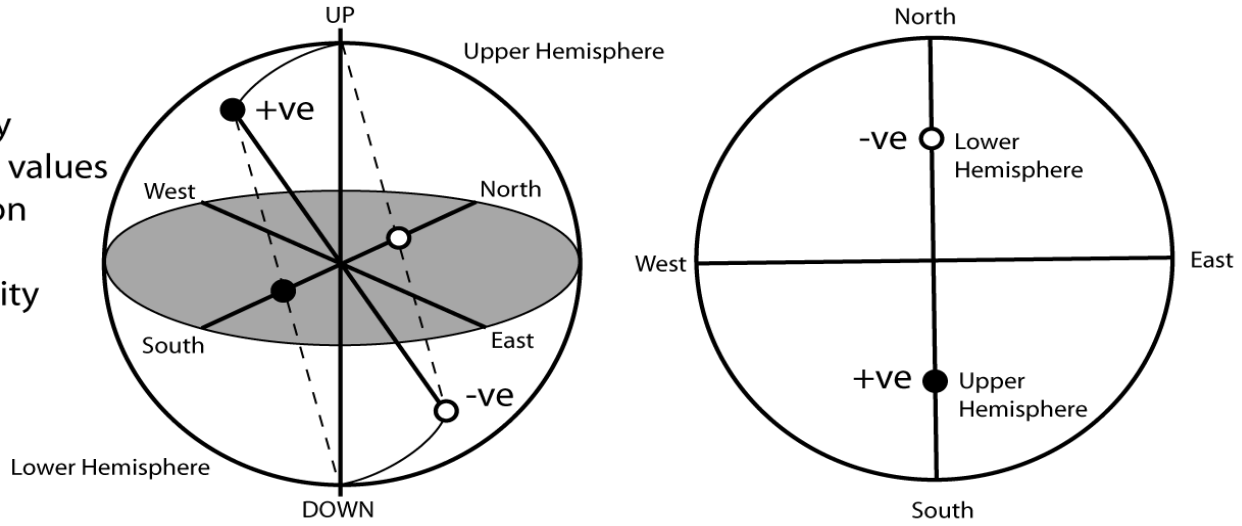

MTEX - Antipodal

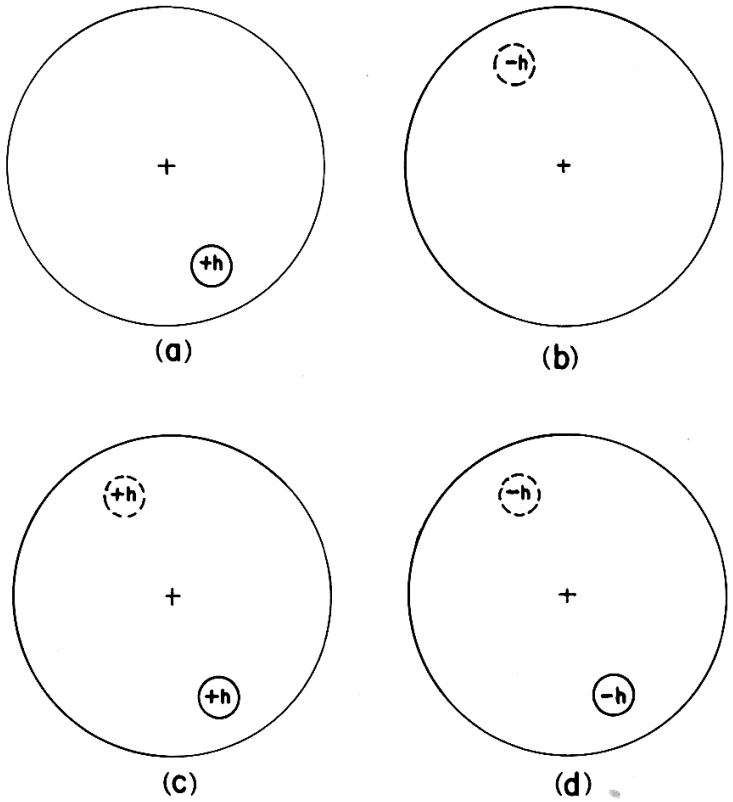

Linear preferred orientations of polar direction $+h$ and $-h$ (diagrammatic). (a) All $+h$ in upper hemisphere. (b) All $-h$ in lower hemisphere. (c) $+h$ directions equally distributed in the two hemispheres. (d) $-h$ directions equally distributed in the two hemispheres.

Inverse Pole figure : sample directions in crystallographic reference x',y',z' axes

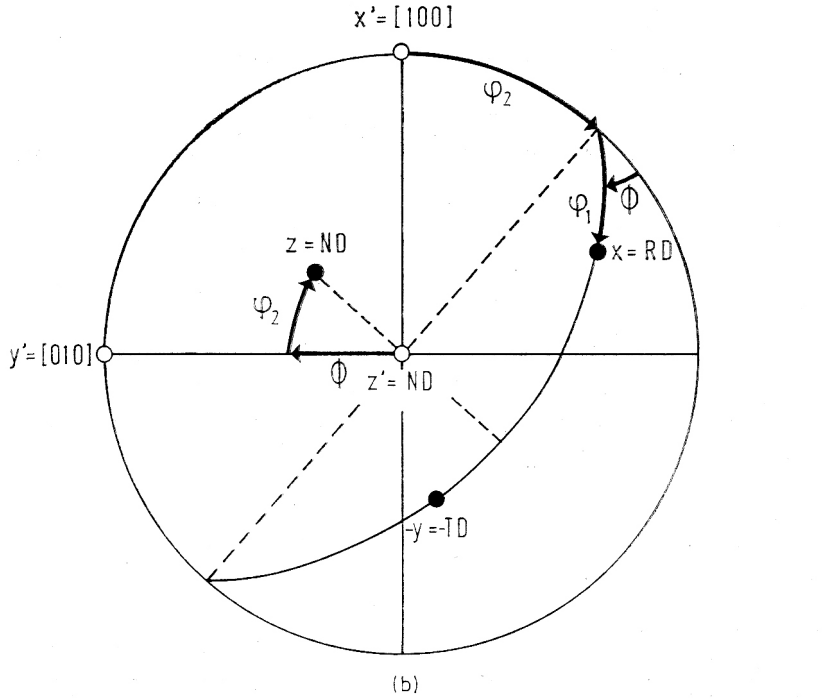

Figure 2.23 The orientation of the sample direction X = RD, Y = TD, Z = ND in the stereographic projection in the crystal coordinate system (inverse pole figure) expressed by the EULER *angles* $\varphi_1 \Phi \varphi_2$

Example of a single crystal

PF and IPF

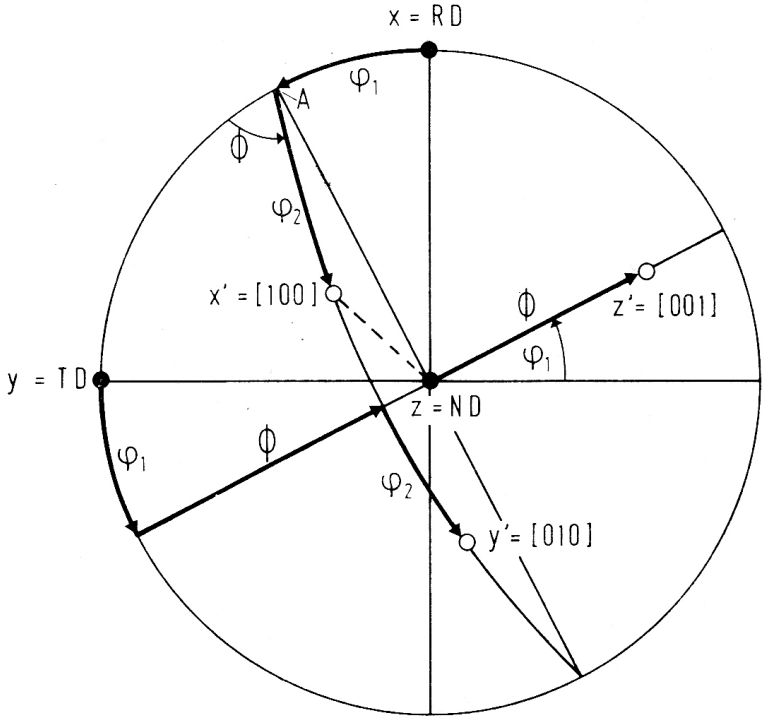

Figure 2.22 The orientation of the crystal directions $X' = [100]$, $Y' = [010]$ $Z' = [001]$ *in the stereographic projection in the sample coordinate system (pole figure) expressed by the* EULER *angles* $\varphi_1 \Phi \varphi_2$

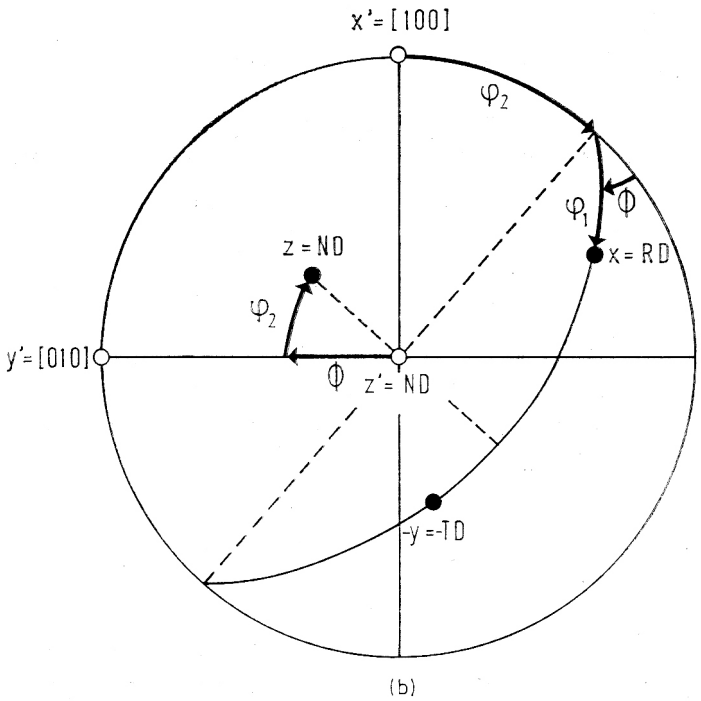

Figure 2.23 The orientation of the sample direction $X =$ RD, $Y =$ TD, $Z =$ ND *in the stereographic projection in the crystal coordinate system (inverse pole figure) expressed by the* EULER *angles* $\varphi_1 \Phi \varphi_2$

Example of a single crystal

PF : hkl // sample direction

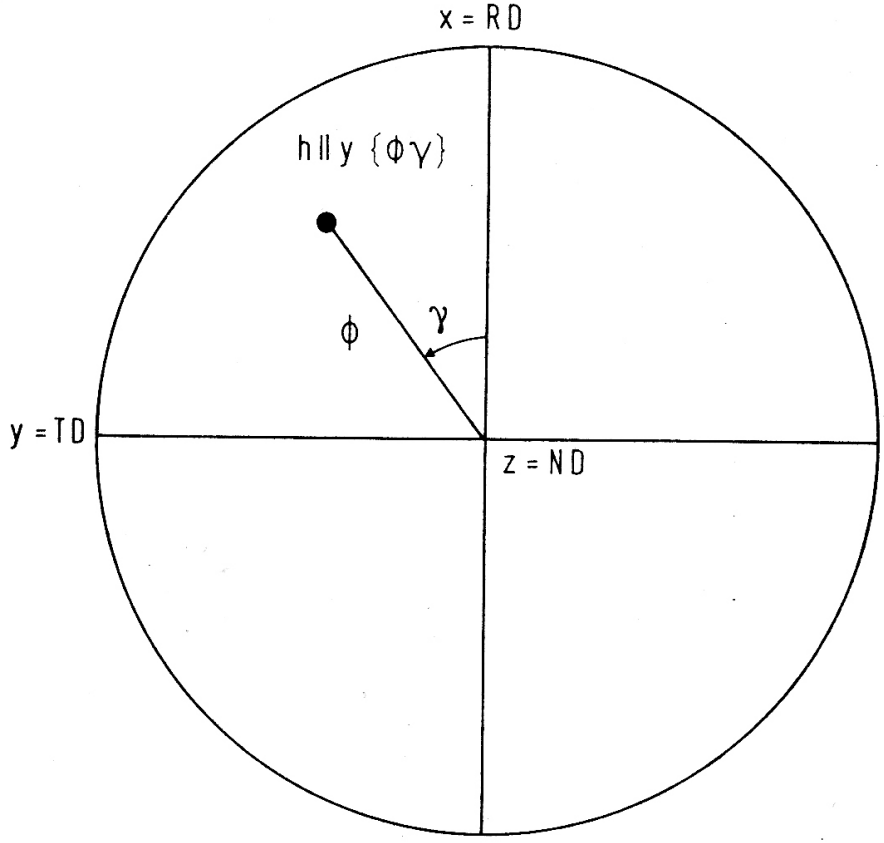

Figure 2.32 Orientation Φγ of a unique crystal direction **h** *relative to the sample fixed* **d** *coordinate system*

IPF : Sample direction // hkl

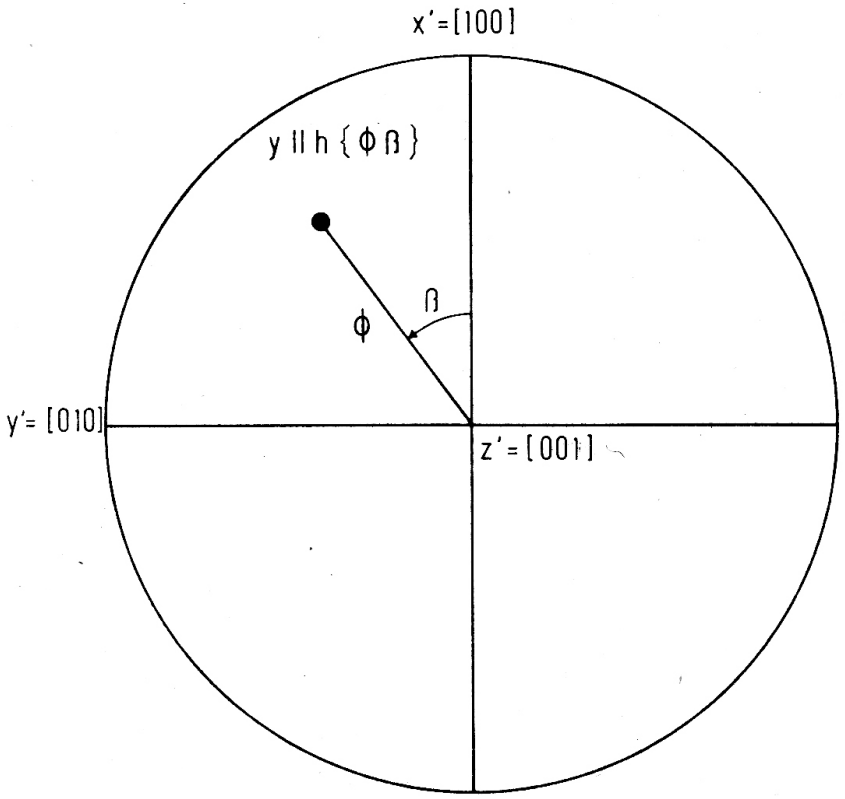

Figure 2.31 Orientation Φβ due to the presence of only one unique sample direction (fibre axis, outer surface normal)

Pole figures

Pole figures

$\mathbf{y} = g^{-1} \cdot \mathbf{h}$

Orientations

$g_n = (\varphi_1, \Phi, \varphi_2)_n$

(n = 1…N)

Inverse pole figures

$\mathbf{h} = g \cdot \mathbf{y}$

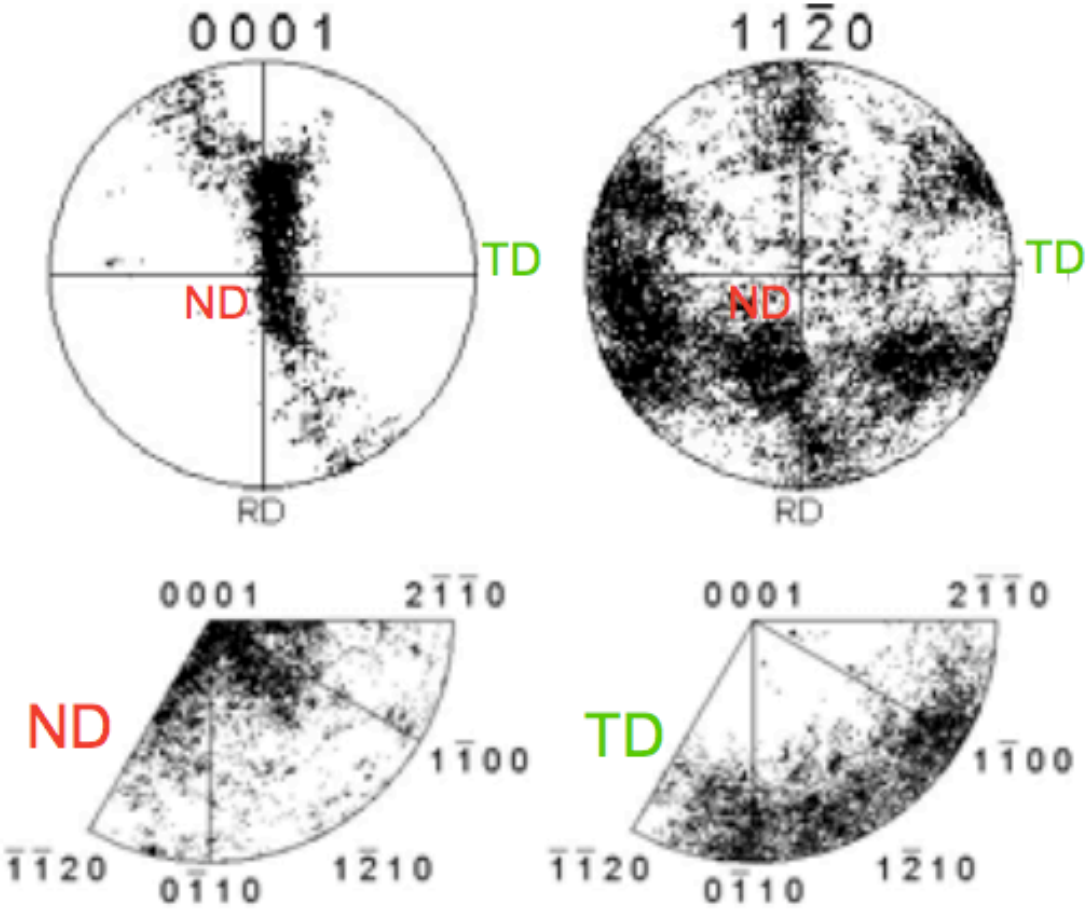

Definition of pole figure & Jpf index

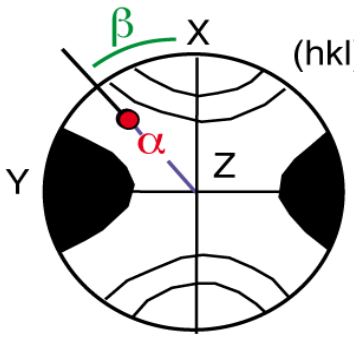

(hkl) = direction in crystal space

$y = \{\alpha\ \beta\}$

$dV/V = f(y)\,dy$

$\int f(y)\,dy = 1$

$dy = d\alpha\, d\beta\, \sin\alpha / x$

for a hemisphere $x = 2\pi$
and a sphere $x = 4\pi$

$$Jpf = \int f(y)^2 dy$$

Definition of inverse pole figure & Jipf index

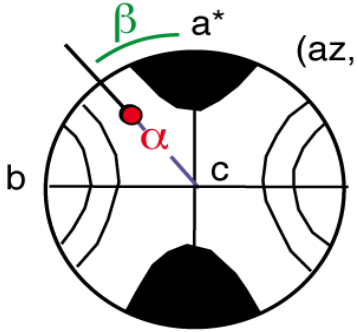

(az,inc) = direction in sample space

$y = \{\alpha\ \beta\}$

$dV/V = f(y)\,dy$

$\int f(y)\,dy = 1$

$dy = d\alpha\, d\beta\, \sin\alpha / x$

for a hemisphere $x = 2\pi$
and a sphere $x = 4\pi$

$$Jipf = \int f(y)^2 dy$$

Misorientation

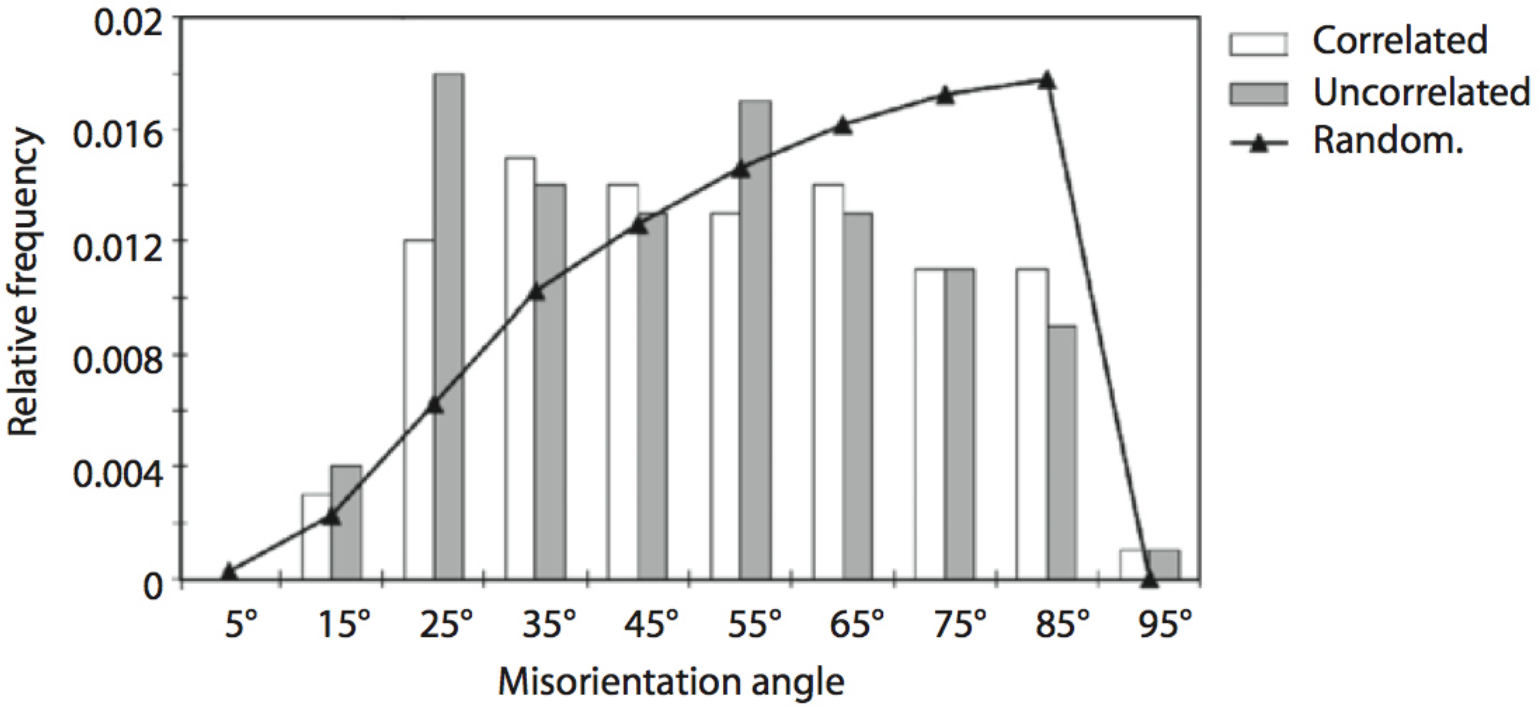

Disorientation angle distribution histogram for correlated and uncorrelated misorientation pairs in commercially pure titanium. The disorientation angle distribution for randomly misoriented crystal pairs is also included (with triangles).

Correlated (neighbour) MODF and uncorrelated MODF

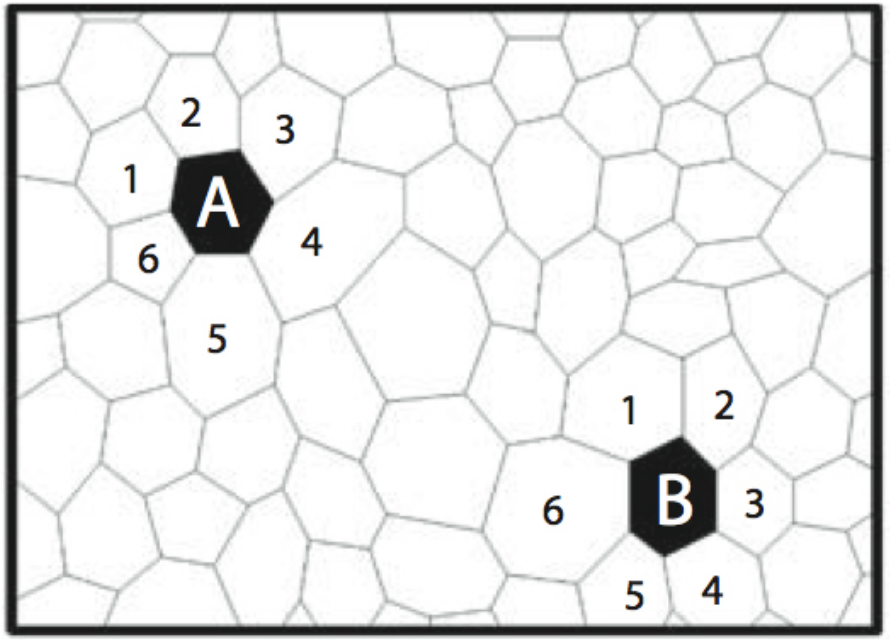

(a)

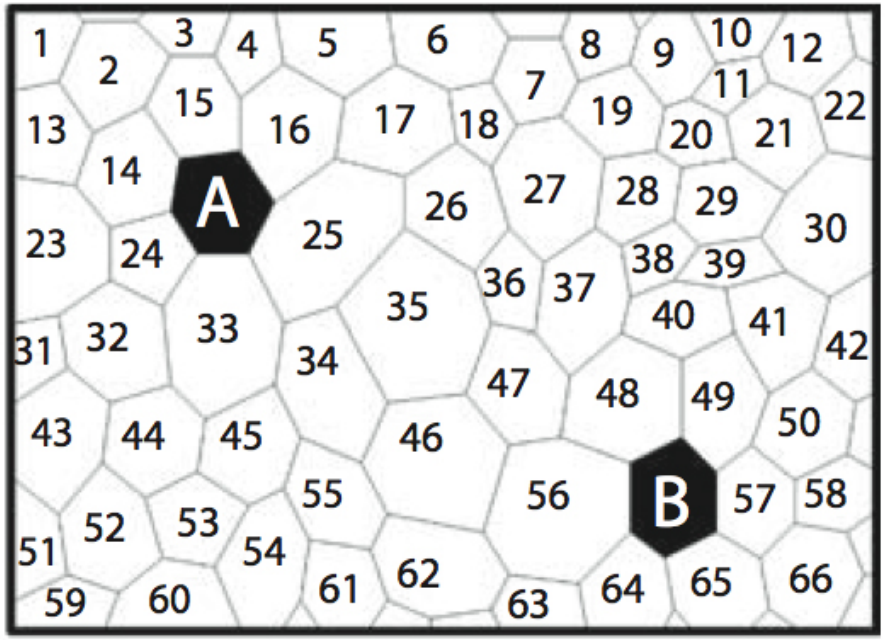

(b)

MODF = MisOrientation DF ODDF = Orientation Difference DF

Schematic sketch of the topological features forming the basis of (a) MODF and (b) ODDF.

DF = Distribution Function

X-ray and neutron diffractometry

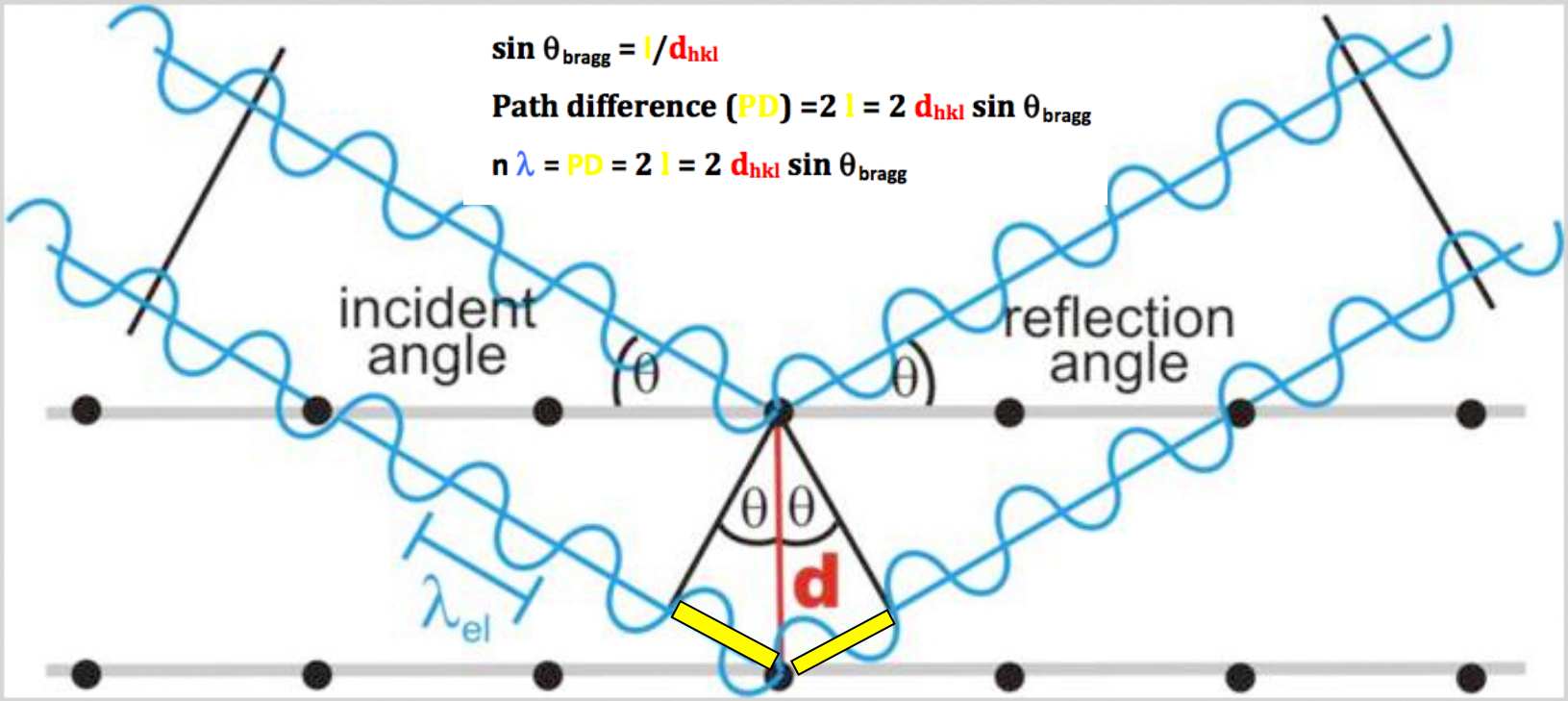

Constructive Interference of reflected waves (reflected waves in phase, i.e., maxima are superimposed).

To obtain constructive interference, the path difference between the two incident and the scattered waves, which is 2dsinΘ, has to be a multiple of the wavelength λ. For this case, the Bragg law then gives the relation between interplanar distance d and diffraction angle Θ:

$$n\lambda = 2d\sin\Theta$$

Average diffraction properties of radiation used for texture measurement by diffraction, with light also included for comparison

	Light	Neutrons	X-rays	Electrons
Wavelength [nm]	400–700	0.05–0.3	0.05–0.3	0.001–0.01
Energy [eV]	1	10^{-2}	10^{4}	10^{5}
Charge [C]	0	0	0	-1.602×10^{-19}
Rest mass [g]	0	1.67×10^{-24}	0	9.11×10^{-28}
Penetration depth, absorption length [mm]	–	10–100	0.01–0.1	10^{-3}

Goniometer Cradle

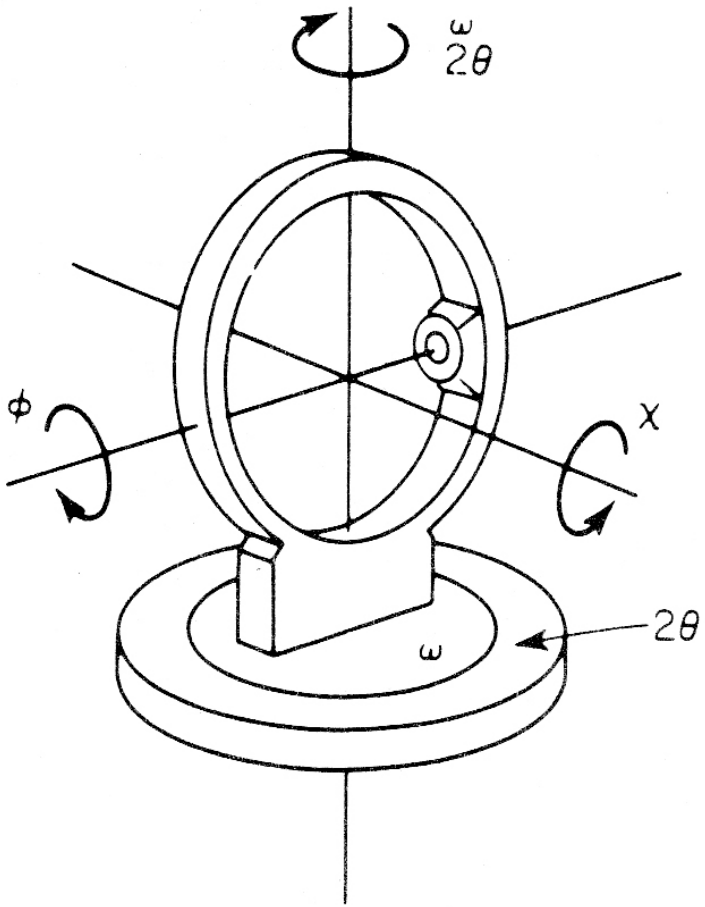

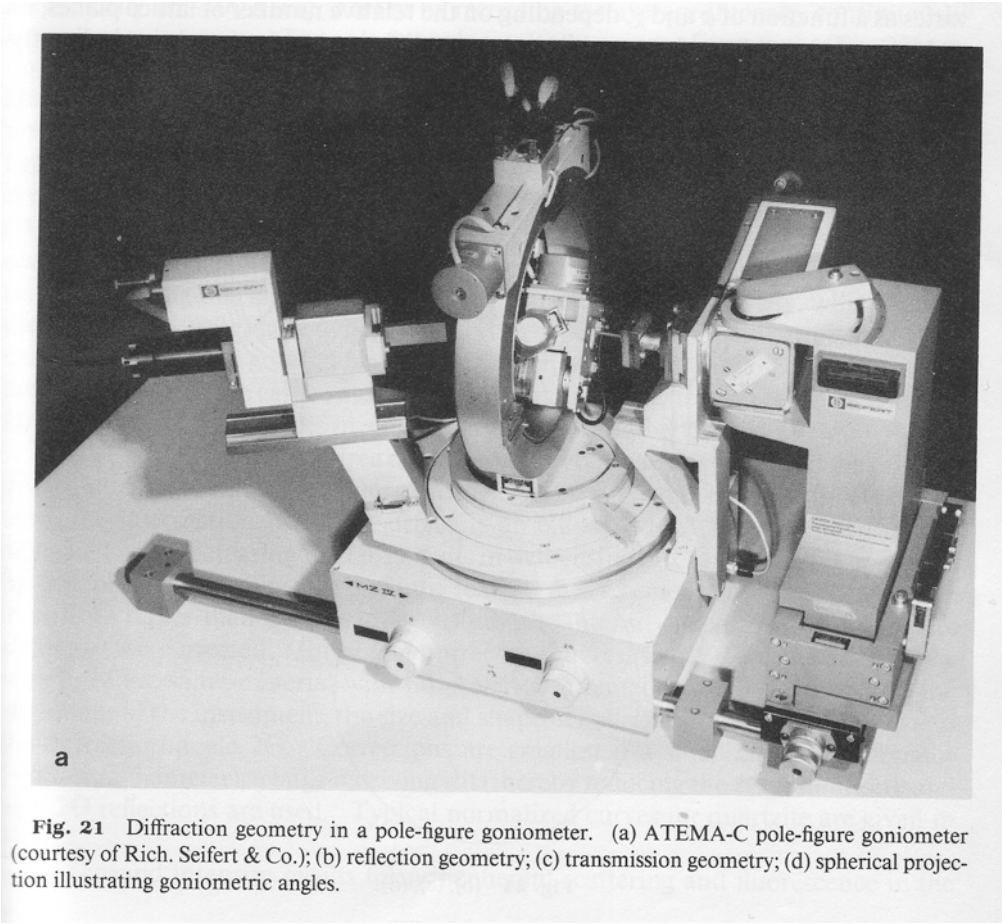

Fig. 21 Diffraction geometry in a pole-figure goniometer. (a) ATEMA-C pole-figure goniometer (courtesy of Rich. Seifert & Co.); (b) reflection geometry; (c) transmission geometry; (d) spherical projection illustrating goniometric angles.

Path difference – dashed line

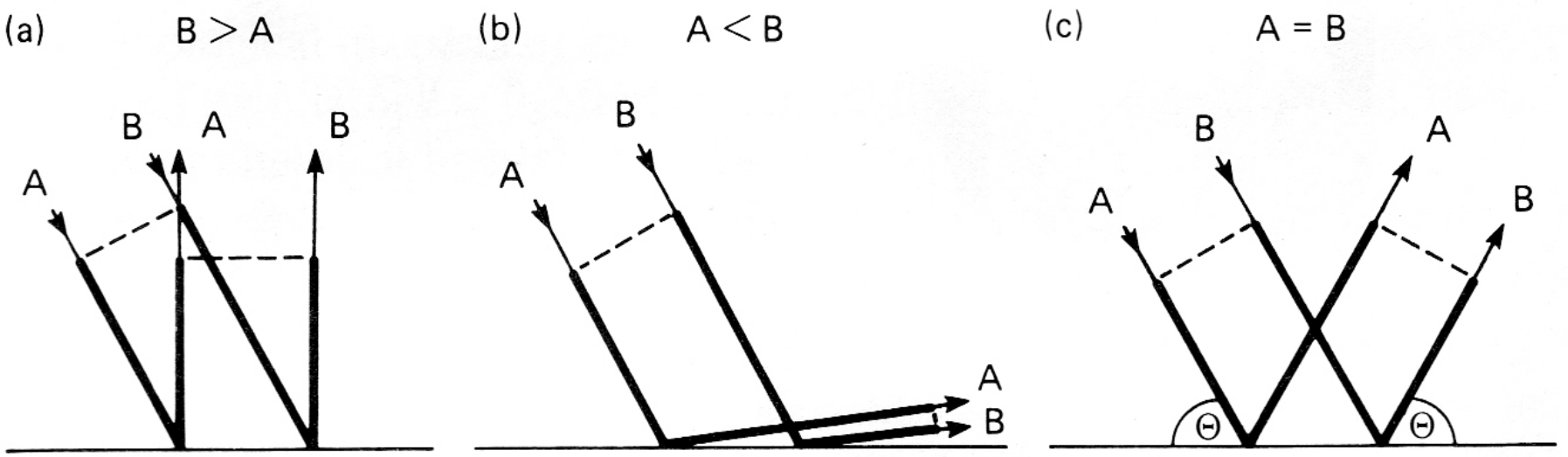

Zero path difference is only attained for reflection geometry (c)

Bragg's Law

$\sin \theta_{bragg} = l/d_{hkl}$

Path difference (PD) $= 2\,l = 2\,d_{hkl} \sin \theta_{bragg}$

$n\lambda = PD = 2\,l = 2\,d_{hkl} \sin \theta_{bragg}$

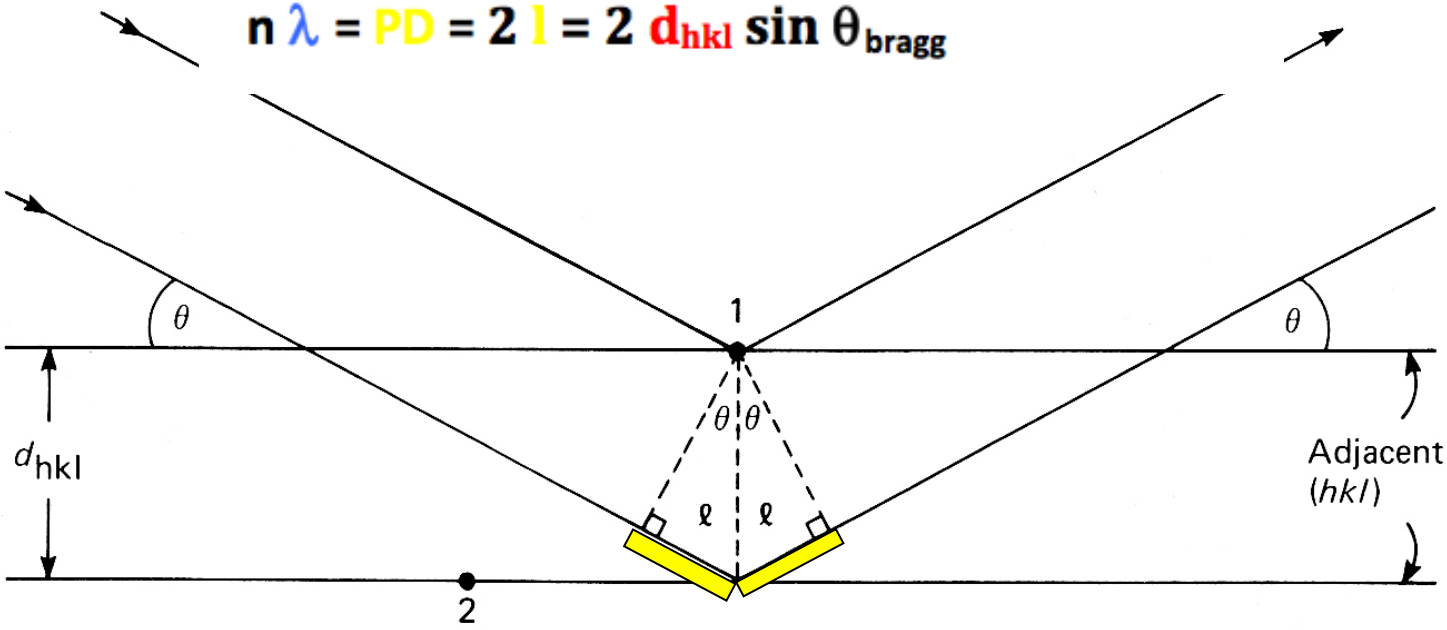

Path difference between adjacent lattice planes (Bragg's law)

Friedel's Law

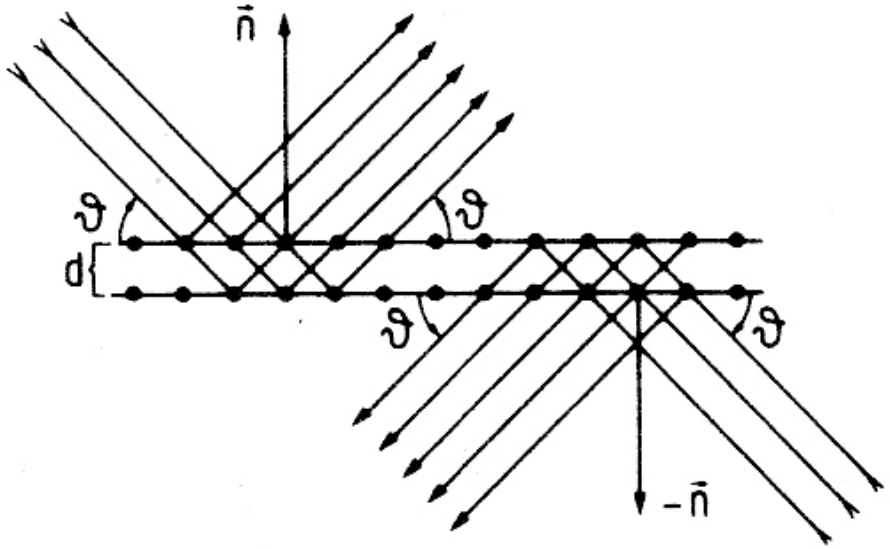

X-ray reflection at both sides
of a set of lattice planes
(Friedel's law)

Diffracting volume

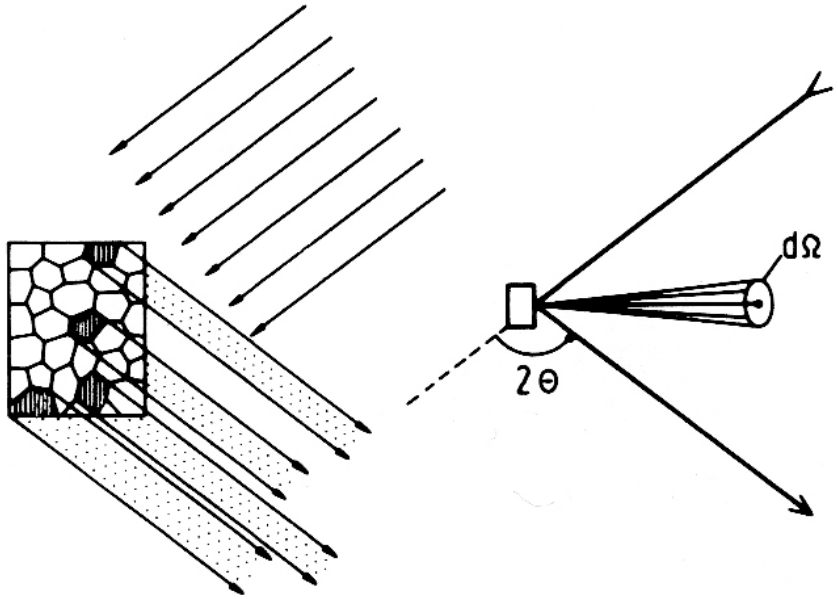

The volume fraction of the material having the crystal direction h parallel to the sample direction y defines the pole density of the h pole figure at the point y.

PF : Relection and Transmission

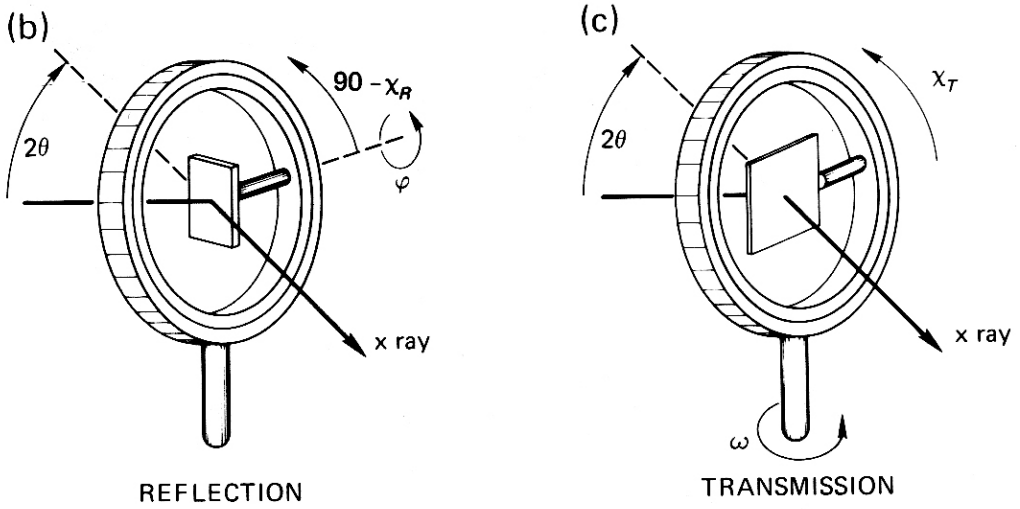

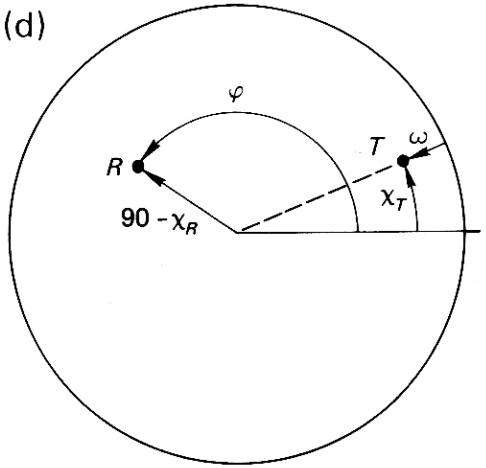

PF : Back-reflection

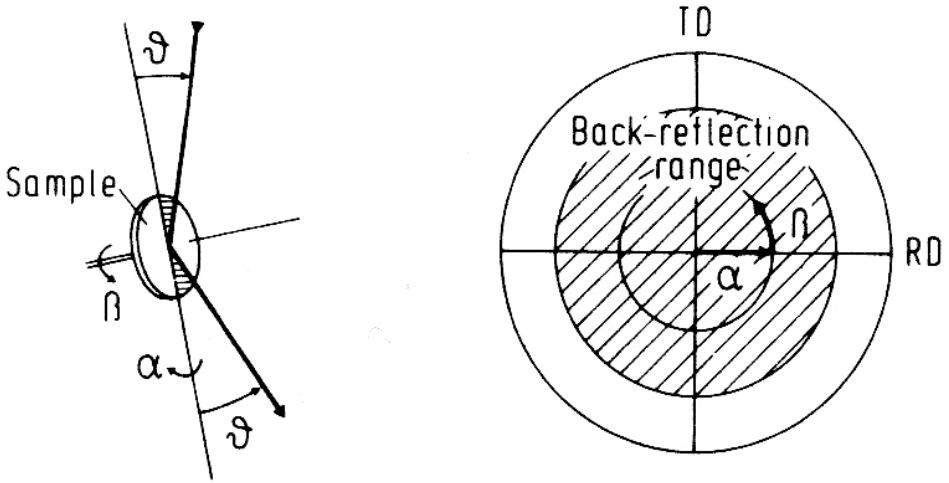

The principles of the back-reflection technique

a - The incident beam and the reflected beam

b - The back-reflection range

PF - Transmission

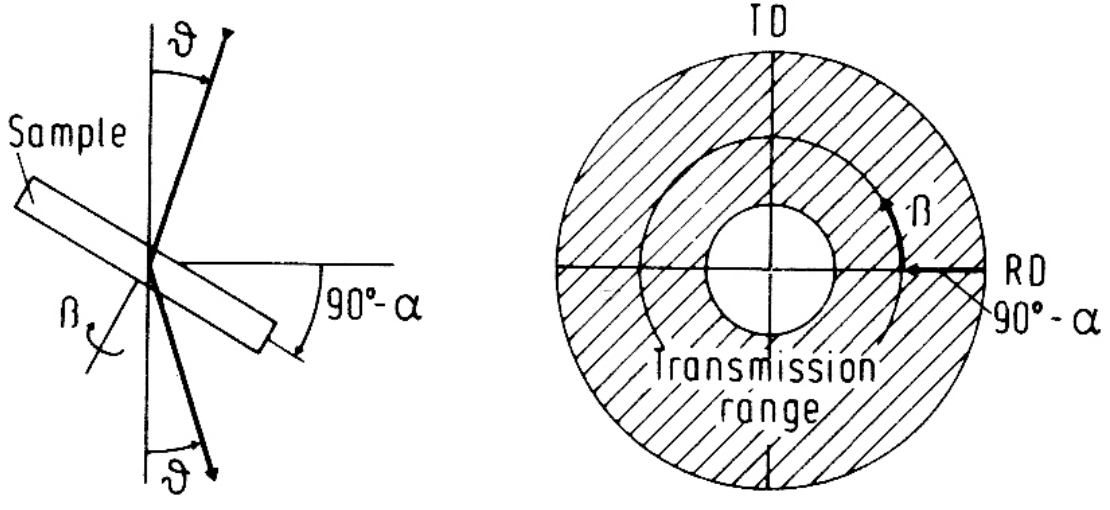

The principles of the transmission technique

a - The incident beam and the reflected beam

b - The transmission range

PF : Reflection -Transmission Overlap

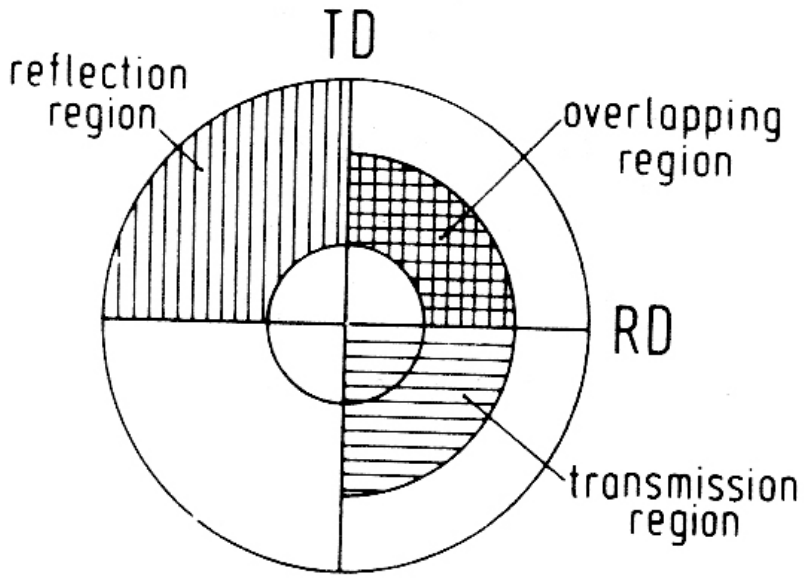

The transmission range, the reflection range and the overlapping range.

Diffraction conditions

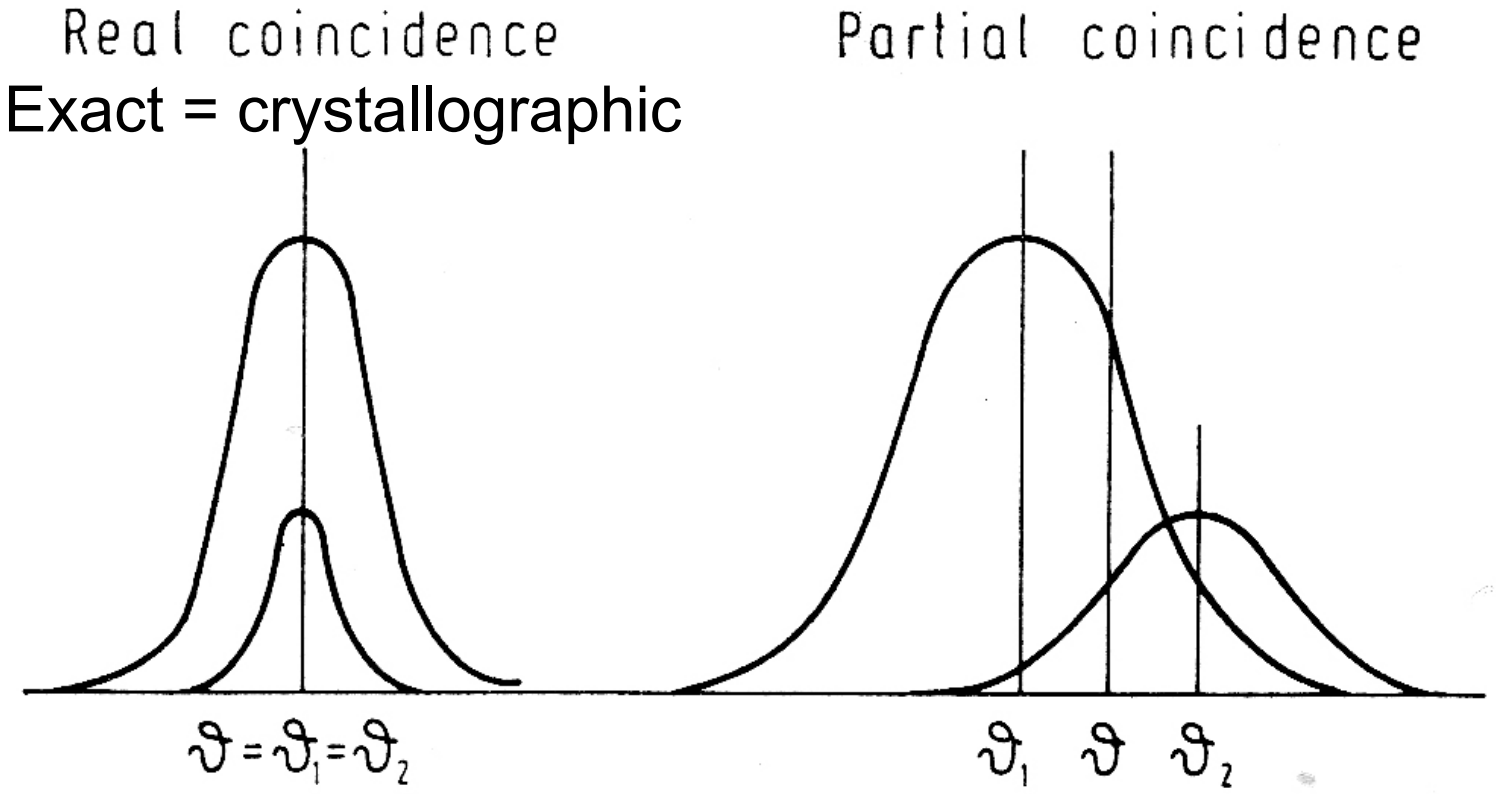

Figure 4.5 Real and partial coincidences

Data need for diffraction measurement

Table 11.3 CRYSTALLOGRAPHIC DATA OF POLE FIGURES FOR QUARTZ

	Diffraction peak $2\theta(CuK_\alpha)$		Indices $hkil$	Crystallographic angles θ	γ	Relative intensity q_{hkil}	Difference $q_{hkil} - q_{khil}$
*	26.7°	1	$10\bar{1}1$	51.8	0.0	0.70	0.40
	26.7°		$01\bar{1}1$	51.8	60.0	0.30	
	36.6°	2	$11\bar{2}0$	90.0	30.0	1	
	42.5°	3	$20\bar{2}0$	90.0	0.0	1	
	45.8°	4	$20\bar{2}1$	68.5	0.0	0.30	0.40
	45.8°		$02\bar{2}1$	68.5	60.0	0.70	
	50.2°	5	$11\bar{2}2$	47.7	30.0	1	
	50.7°	(6)	0003	0.0	0.0	1	
	60.0°	7	$21\bar{3}1$	73.4	19.1	0.54	0.08
	60.0°		$12\bar{3}1$	73.4	40.9	0.46	
	64.1°	8	$11\bar{2}3$	36.2	30.0	1	
	73.5°	9	$10\bar{1}4$	17.7	0.0	0.22	0.56
	73.5°		$01\bar{1}4$	17.7	60.0	0.78	
						mean value	0.36

Intensity Corrections

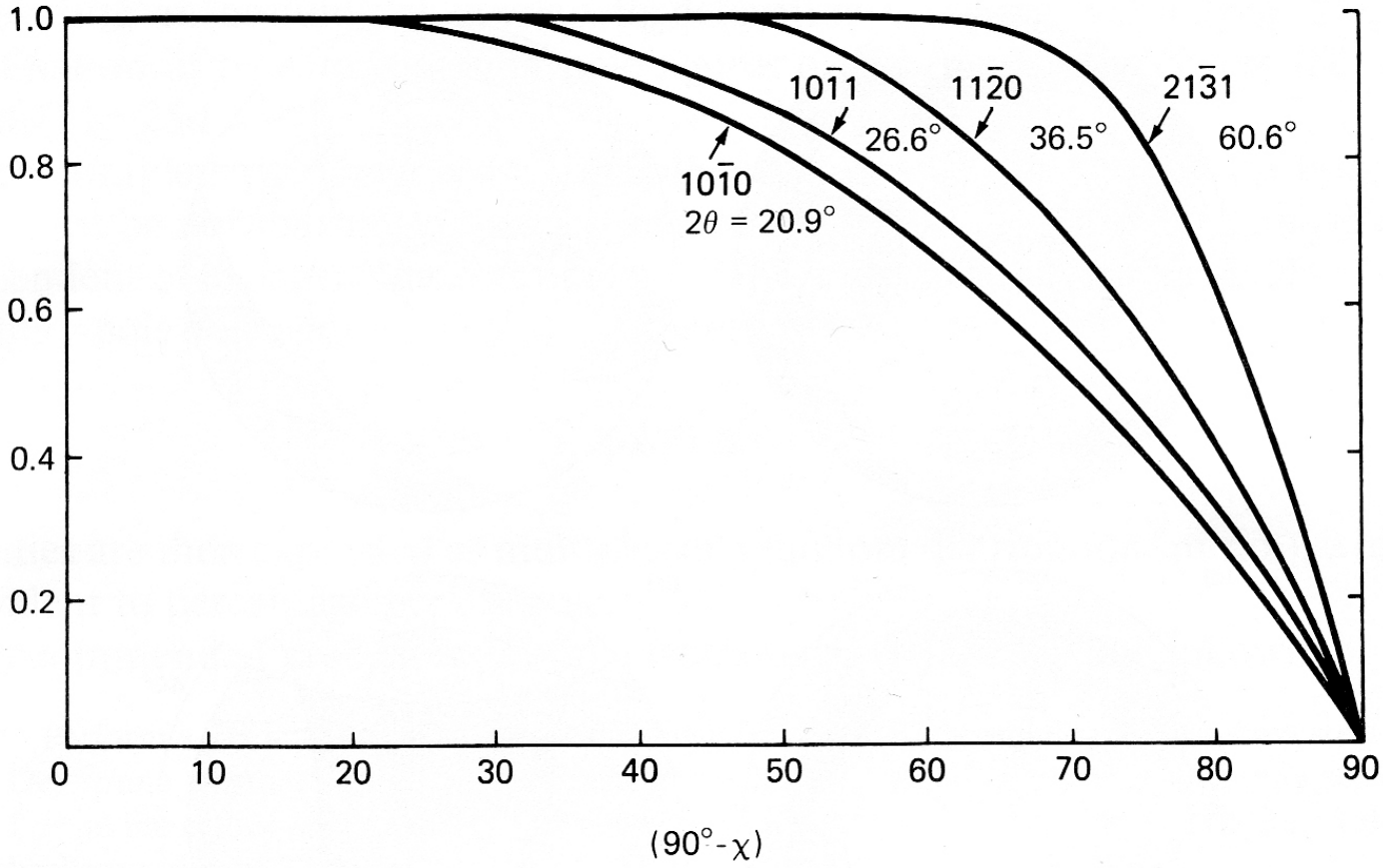

Intensity correction for x-ray pole-figure determinations in reflection geometry. Selected reflections of quartz. Cu *Kα* radiation (from Baker *et al.*, 1969)

Over-lapping 2 theta peaks

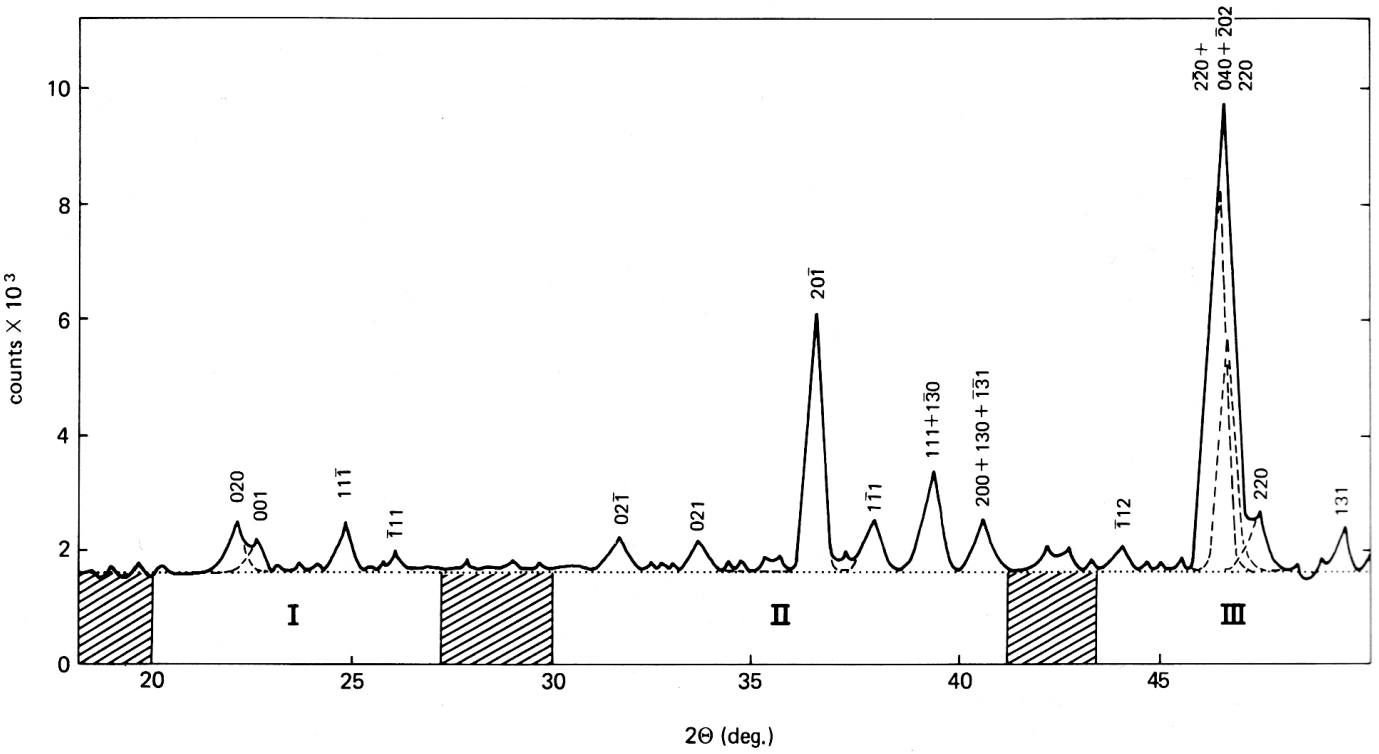

Fig. 27 2Θ profile of anorthosite from San Juan Bautista, California, measured with a 2Θ position-sensitive detector and neutron radiation. In regions I, II, and III deconvolution into gaussiens was performed. Solid line: measured profile; dashed: fitted curve; dotted: background (Bunge *et al.*, 1982a and courtesy of E. Jansen).

Solid angle 2-theta detector

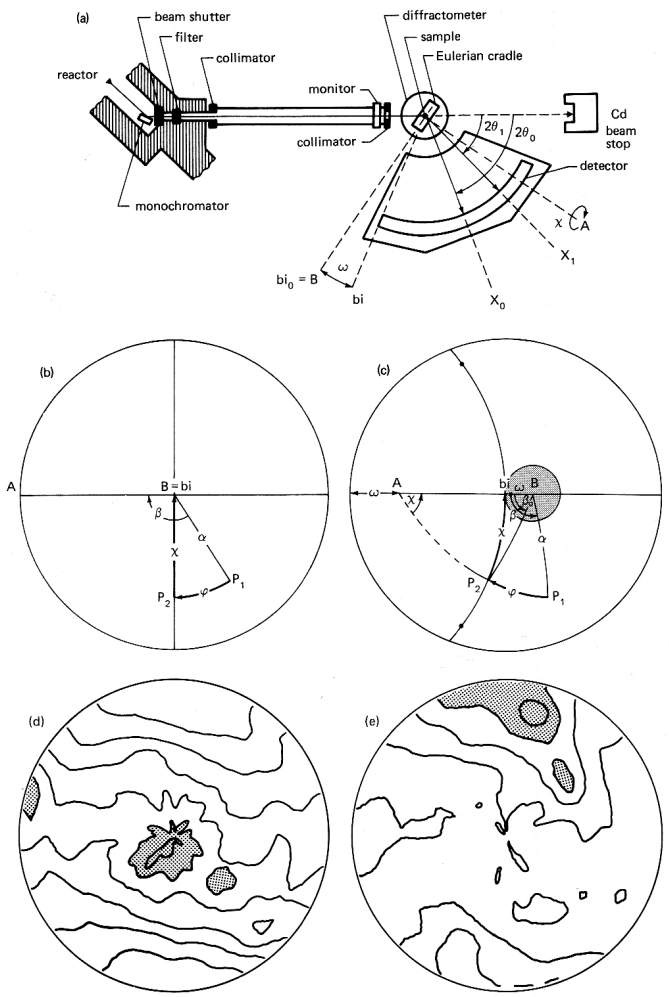

Fig. 28 Continuous detector with neutron diffraction. (a) shows the setup, (b) illustrates angular relations for bisecting geometry and contrasts them with an asymmetric detector position (c). (d,e) Two pole figures of plagioclase in anorthosite (same sample as in Fig. 27) obtained with a 2Θ continuous detector, (d) ($\bar{1}12$), (e) ($1\bar{3}1$). Contour interval 0.25 m.r.d., shaded above 1.5 m.r.d.

X-ray pole figure inversion program !

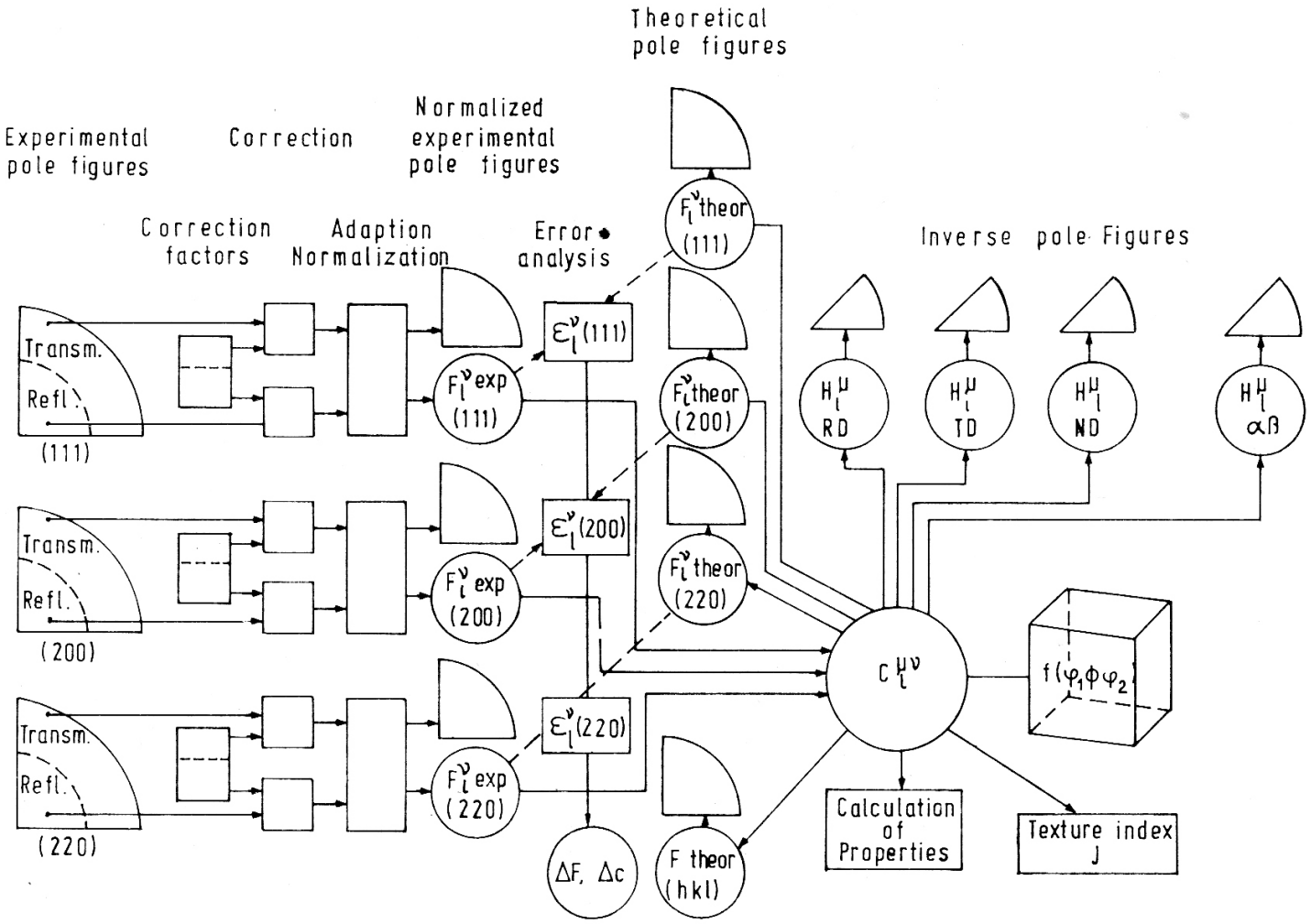

Figure 9.3 Structure of the texture analysis program system[171]

Harmonic Method

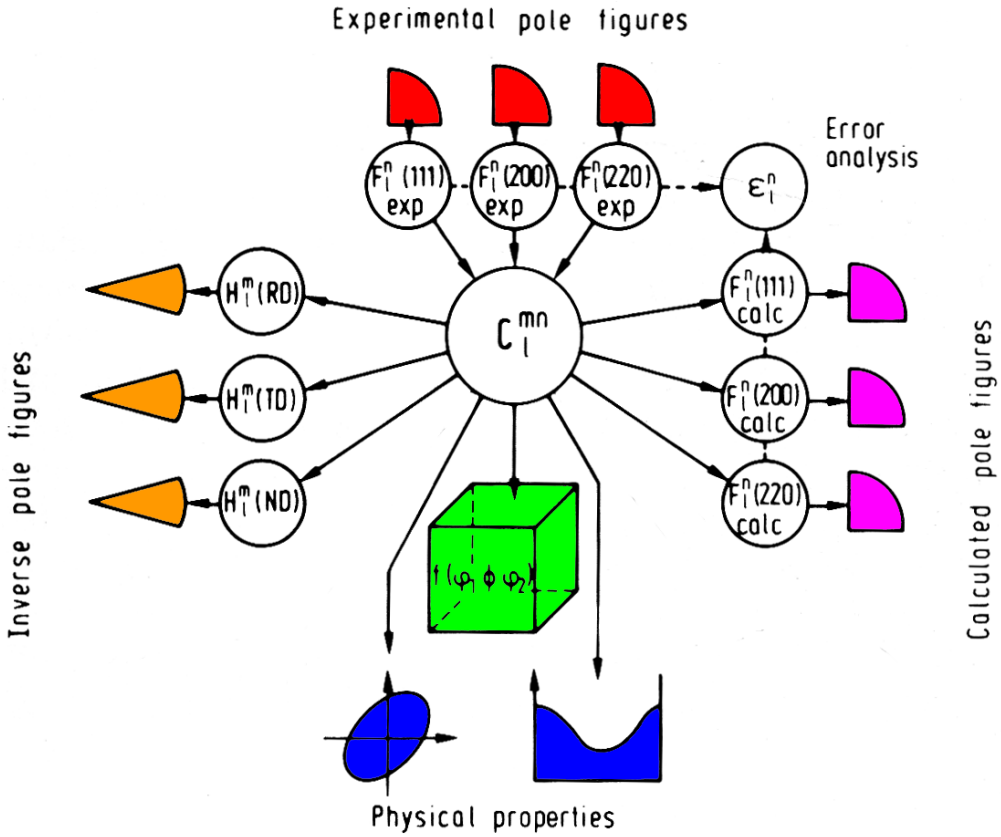

The general scheme of harmonic texture analysis.

X-ray and Neutron diffraction

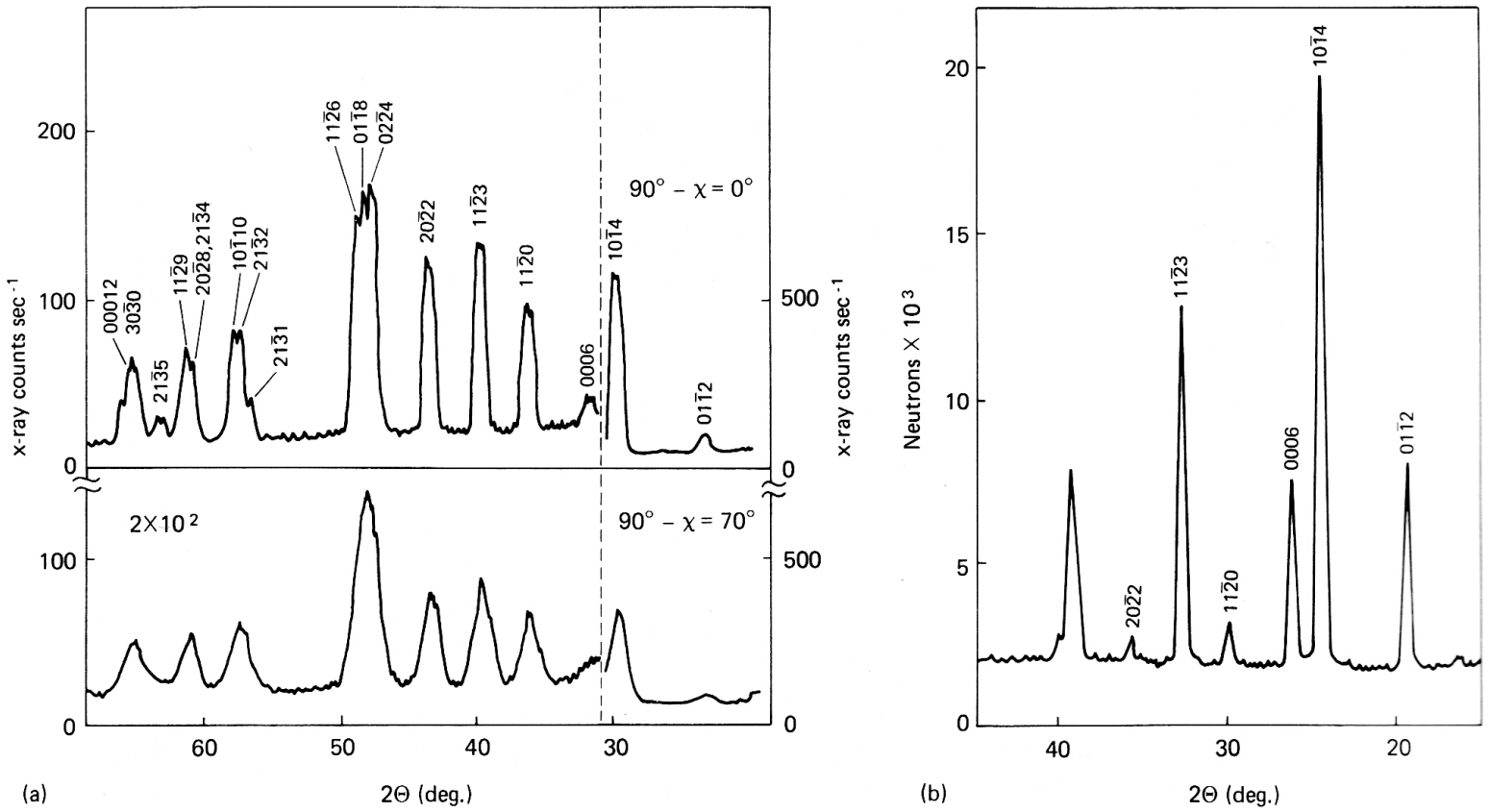

2Θ scans of a limestone specimen in reflection geometry. (a) X-ray Cu $K\alpha$ radiation at $\chi = 90°$ and at $\chi = 20°$ with line broadening. (b) is a comparative neutron diffraction pattern. Note the different intensity distribution.

Quartz : recalculated X-ray pole figures

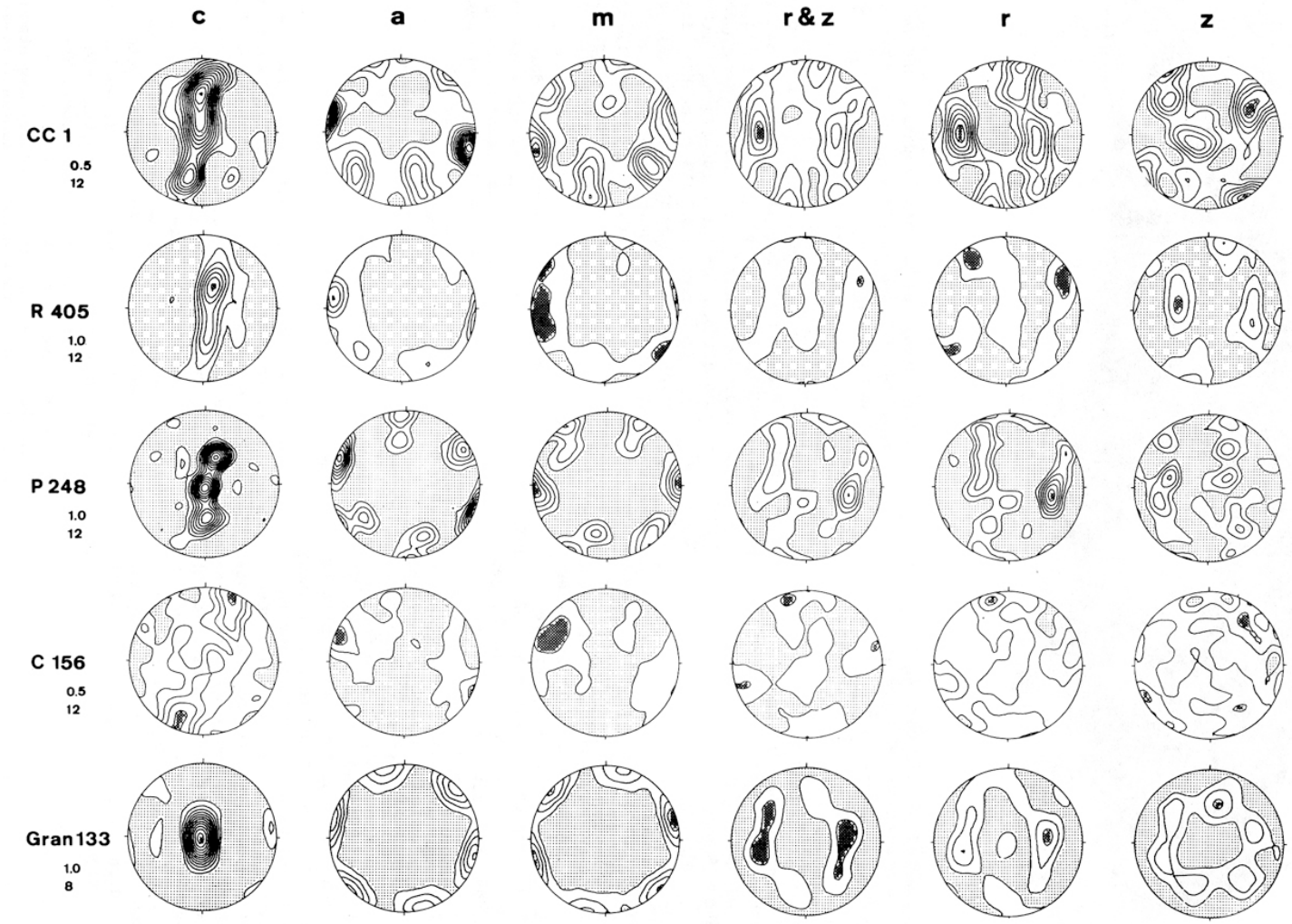

Analysis using ODF

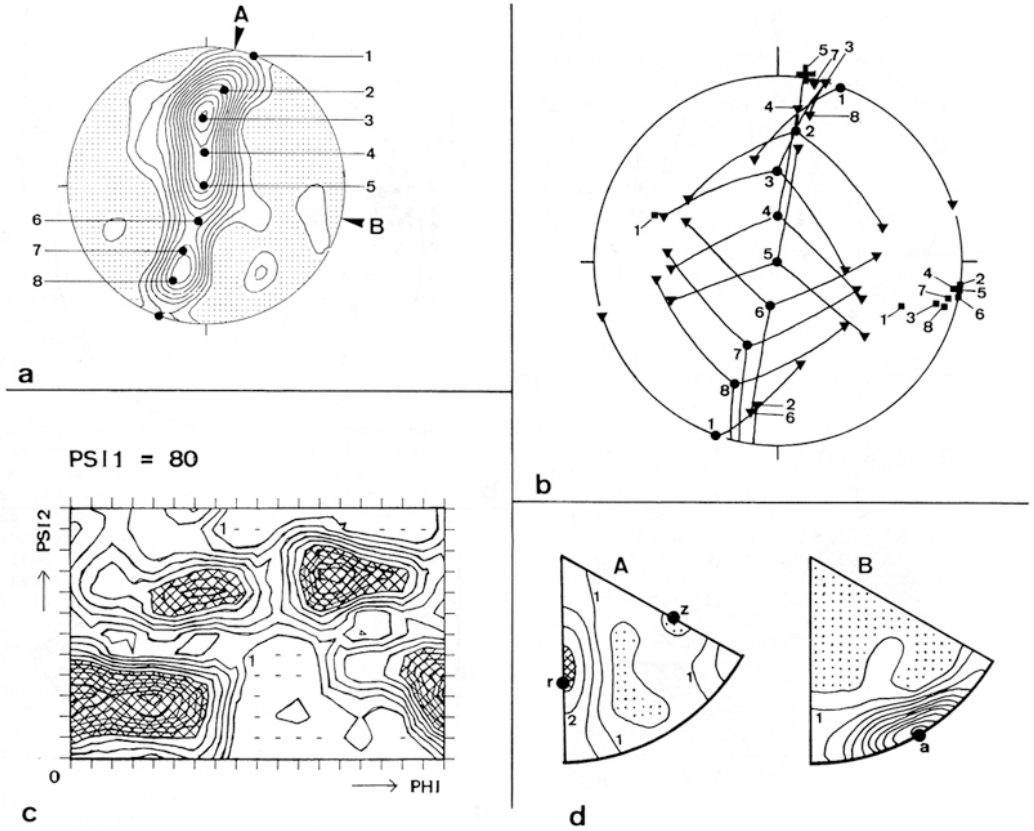

Fig. 6. Analysis of specimen CC 1.

a: Pole figure for the c-direction (contour interval 1.0) indicating and numbering the c-axis positions of crystal orientations chosen for the construction in figure 6b. Specimen directions A (normal to the shear plane) and B (shearing direction) were used for the calculation of the inverse pole figures shown in figure 6d.

b: Favoured crystal orientations for selected c-axis positions shown in figure 6a. Dots: c-axis; triangles: poles to the positive rhombs; squares: one of the three ⟨a⟩ directions, closely aligned with the B specimen direction; cross: pole to the first order prism of c-axis position 5.

c: Section through the three-dimensional graphical representation of the ODF. Order of expansion: 10; contour interval: 1.0. Dashes indicate crystal positions with probabilities calculated to be negative. Crosshatched area: probability higher than 6.0.

d: Inverse pole figures for the specimen directions A and B (see figure 6a). Order of expansion: 12; contour interval: 0.5. A crystal projection with the c-axis in the centre was chosen, and the positions of the r, z and a-directions are indicated.

Synchrotron = new high brilliance x-rays source

ESRF - Ring

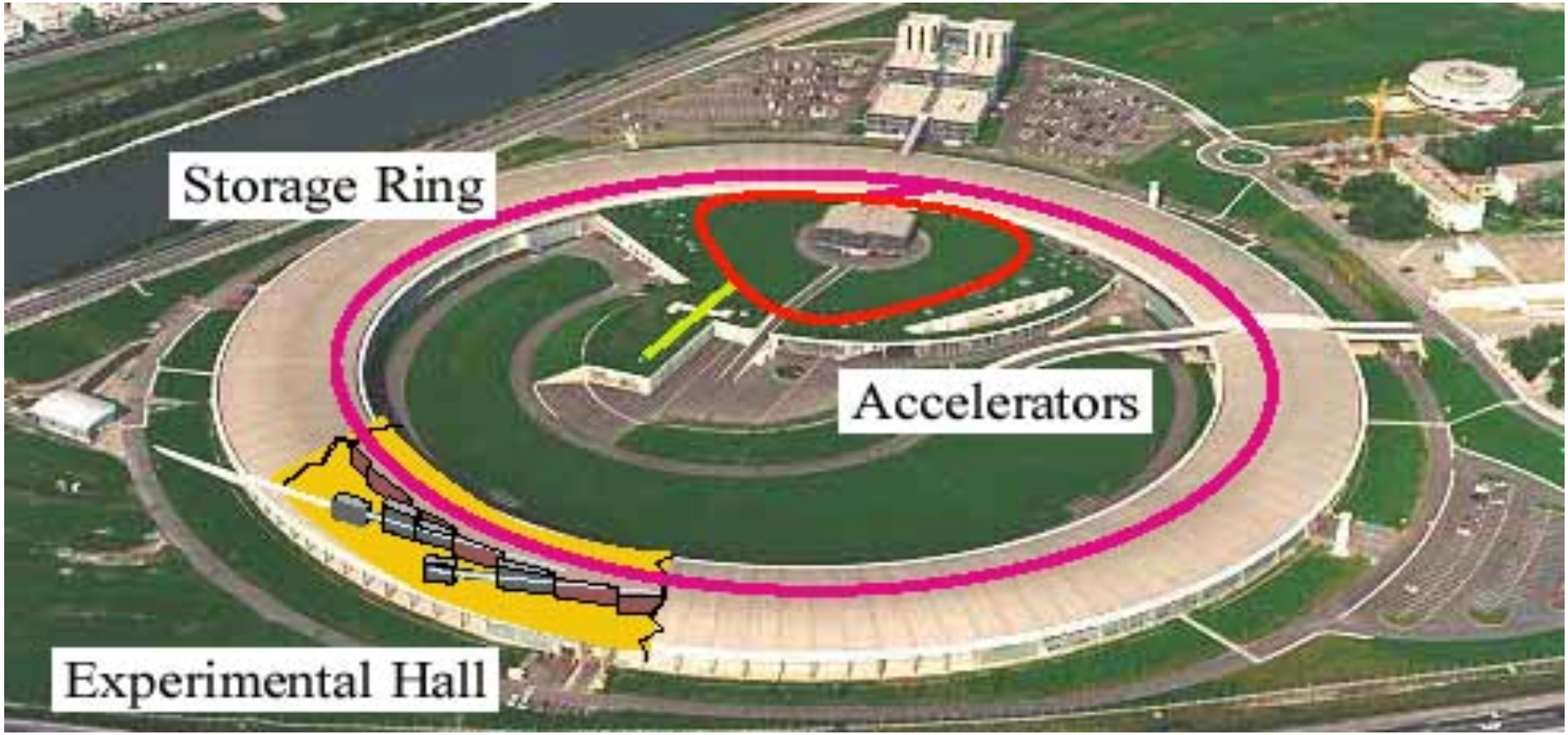

ESRF Brilliance

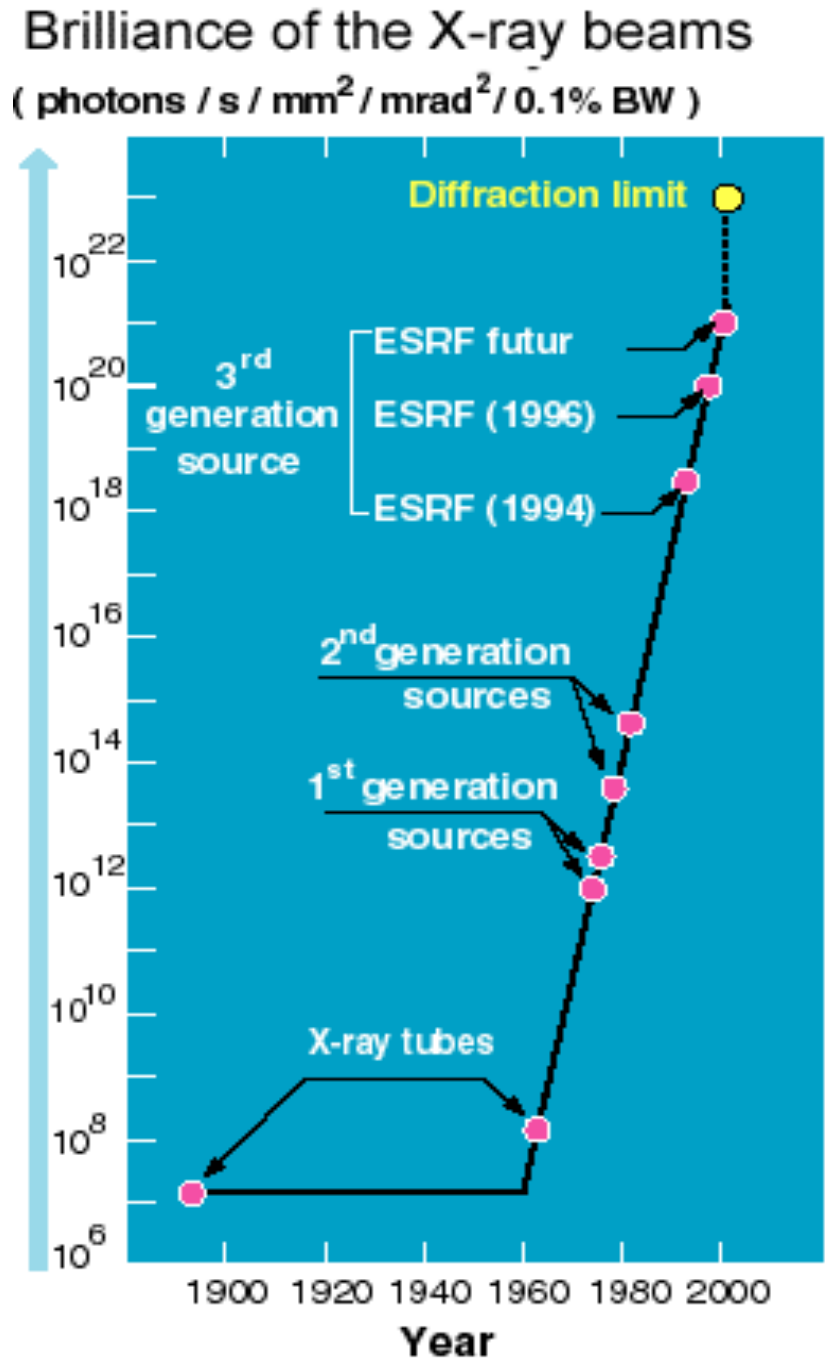

ESRF Beam

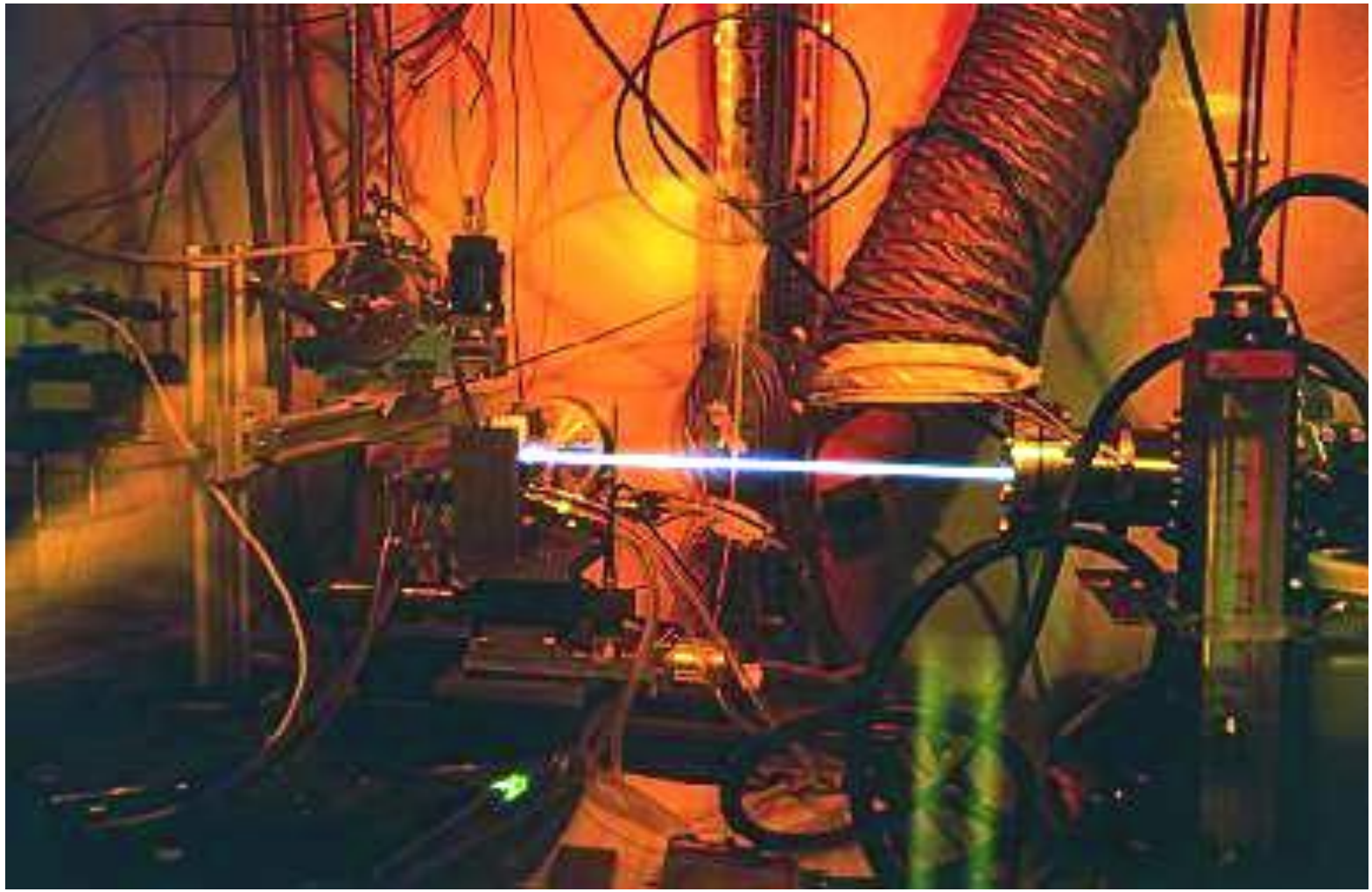

2D plate – in situ high pressure

Orientations préférentielles

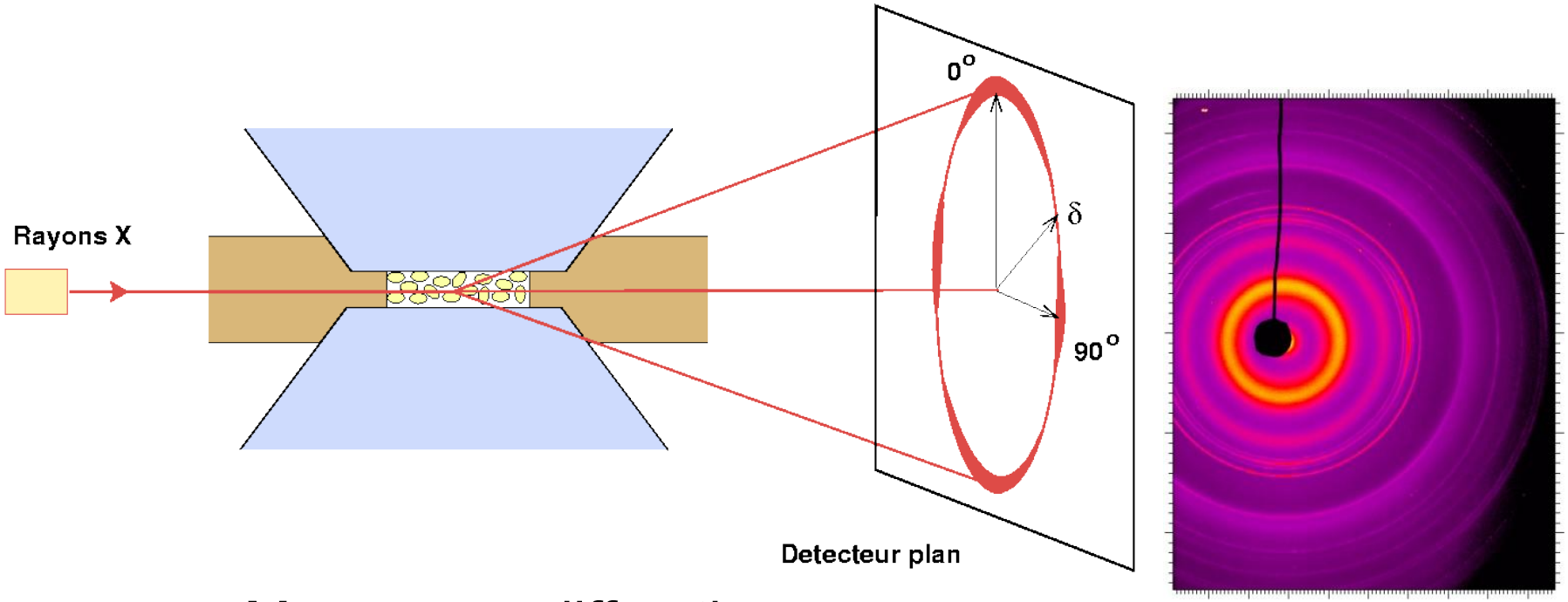

Mesure par diffraction

Preferred orientation in MgO

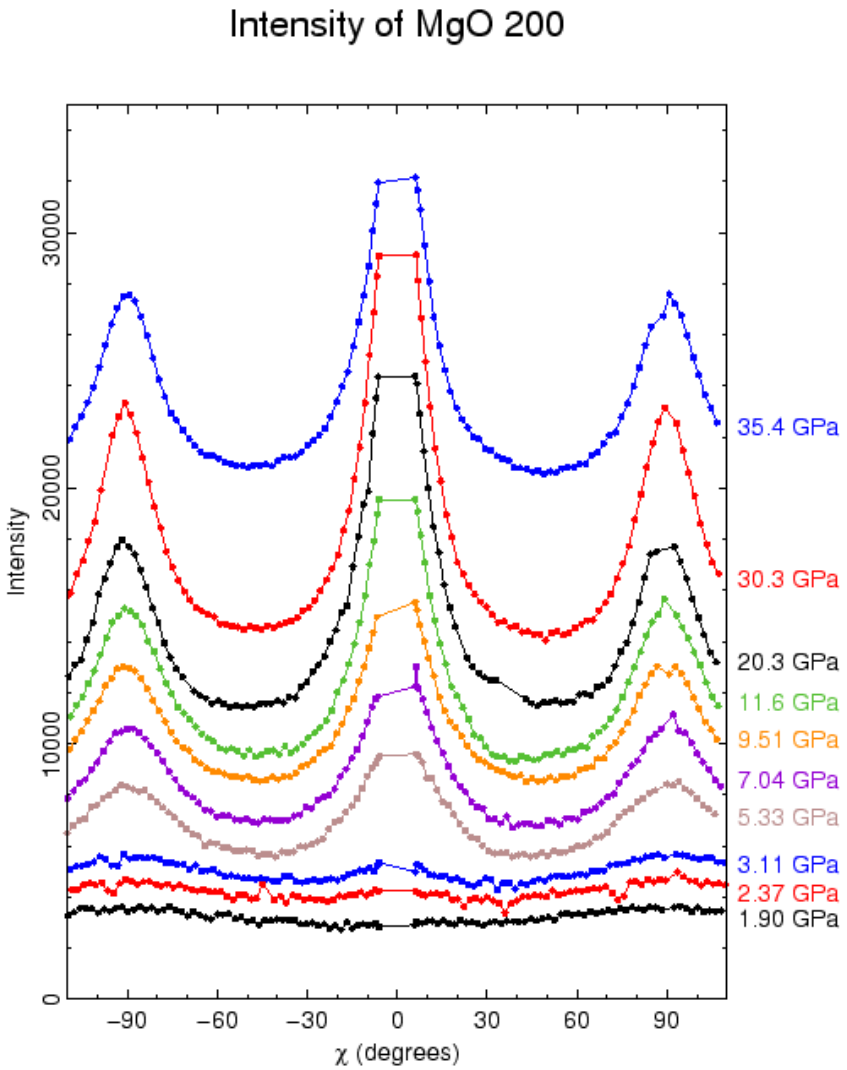

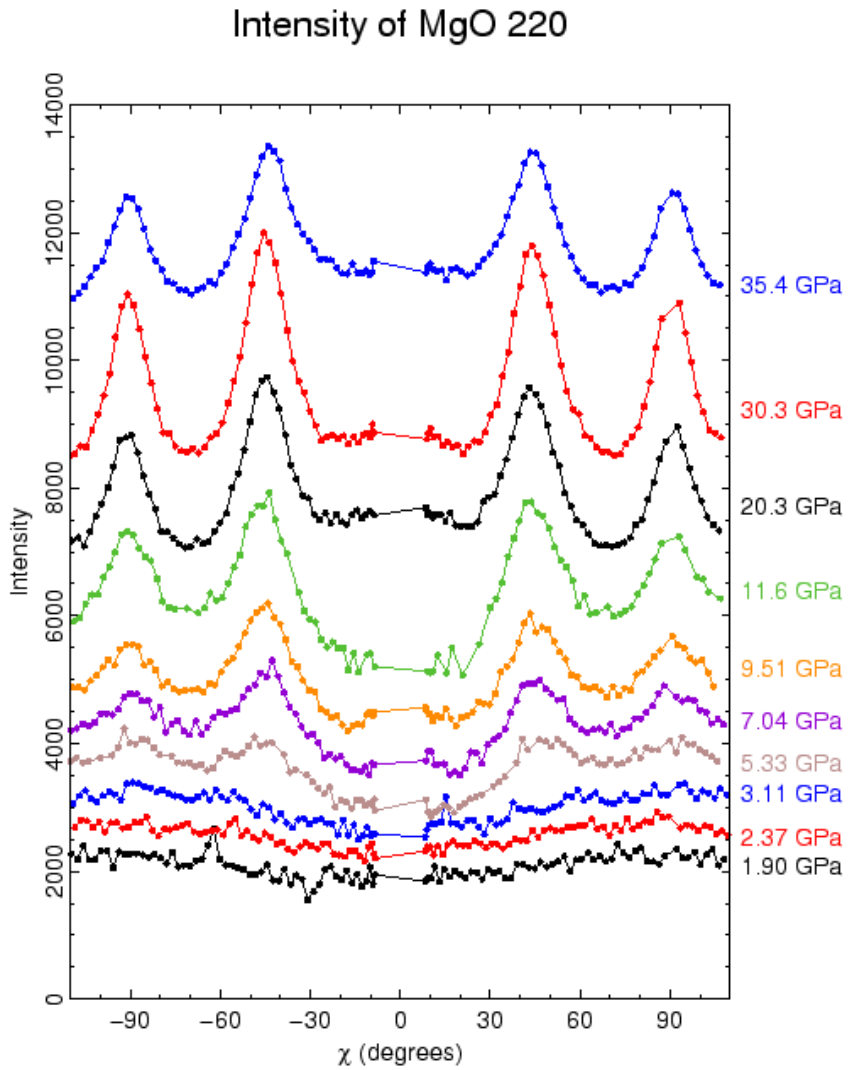

S. Merkel *et al*., J. Geophys. Res., in press

Texture evolution with compression

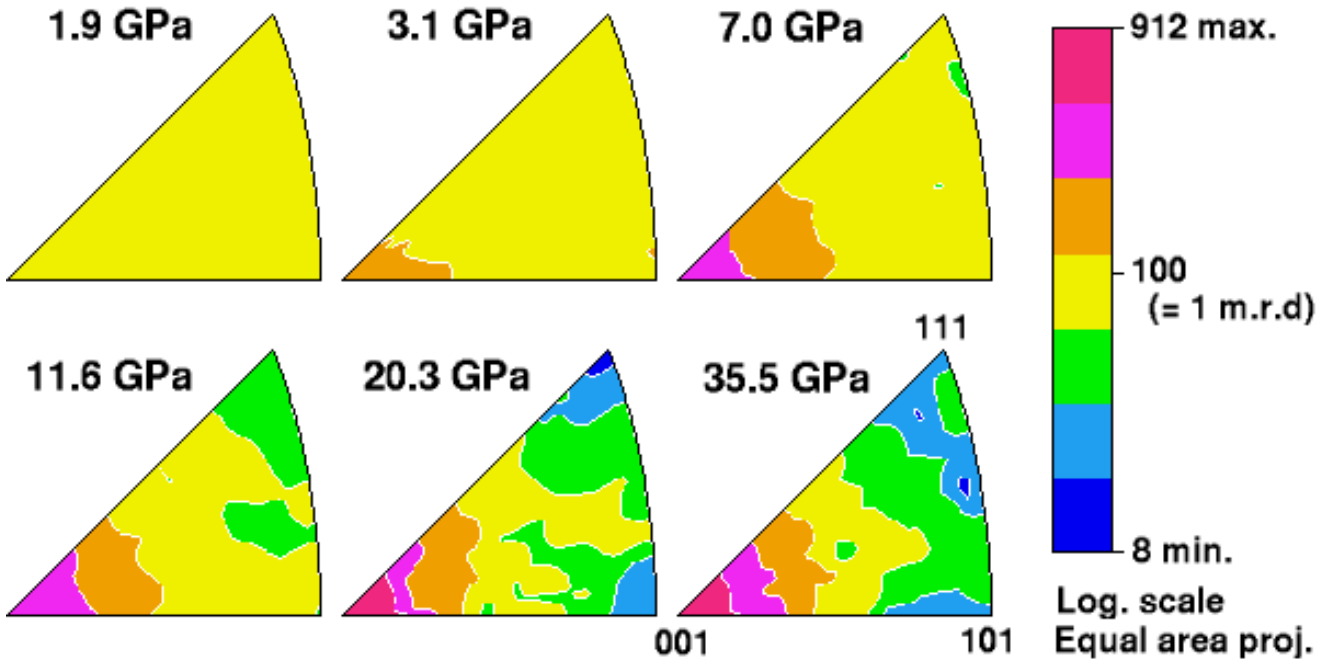

Self consistent polycristal plasticity modeling - soft {110}<110> slip system is the most active

S. Merkel *et al*., J. Geophys. Res., in press

Transmission : Synchrotron X-ray diffraction

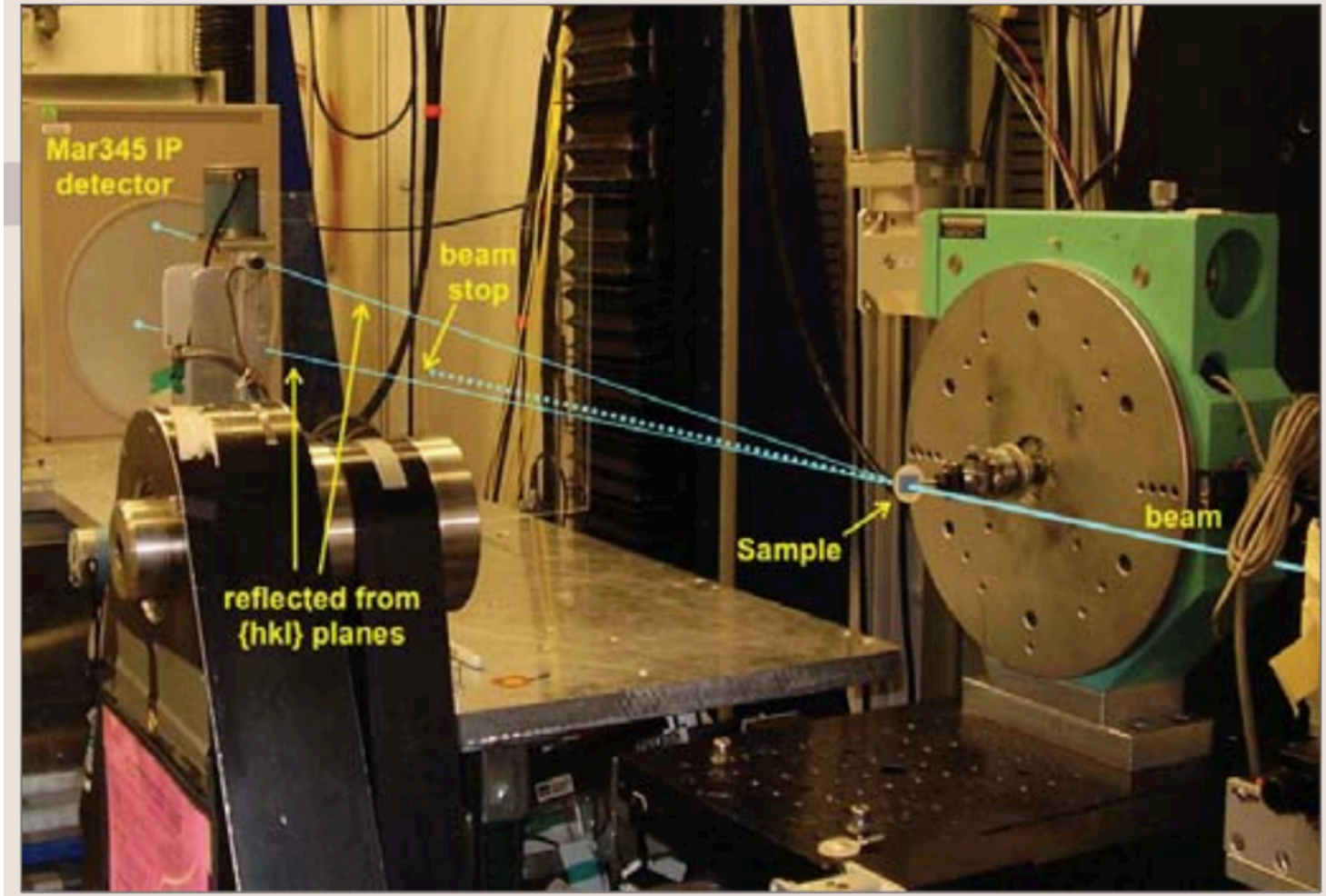

Figure 1. *Experimental setup at the Advanced Photon Source (beamline 11–ID-C) for the synchrotron X-ray texture measurements.*

2D Diffraction plate (false colour)

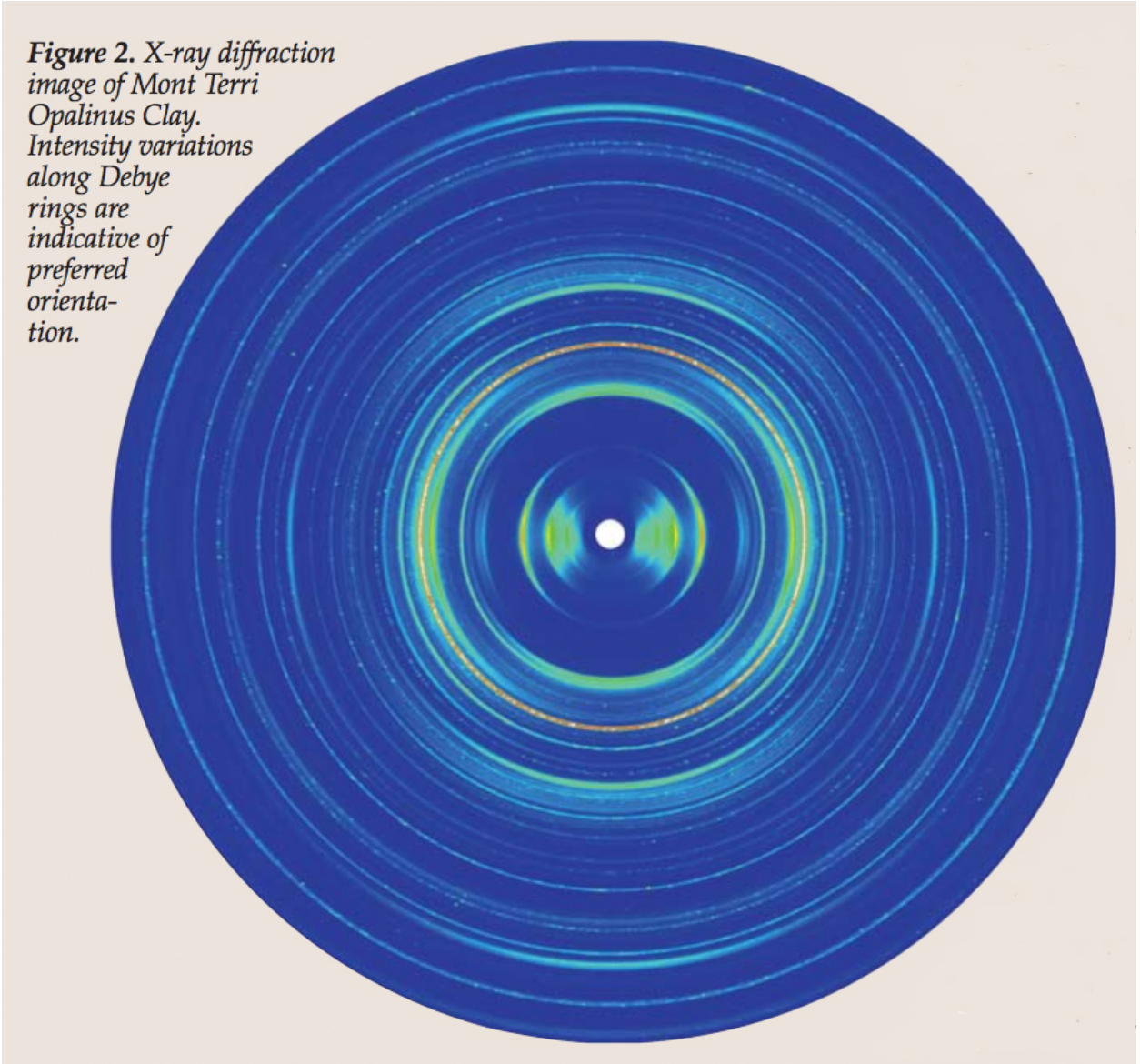

Figure 2. *X-ray diffraction image of Mont Terri Opalinus Clay. Intensity variations along Debye rings are indicative of preferred orientation.*

Rietveld refinement

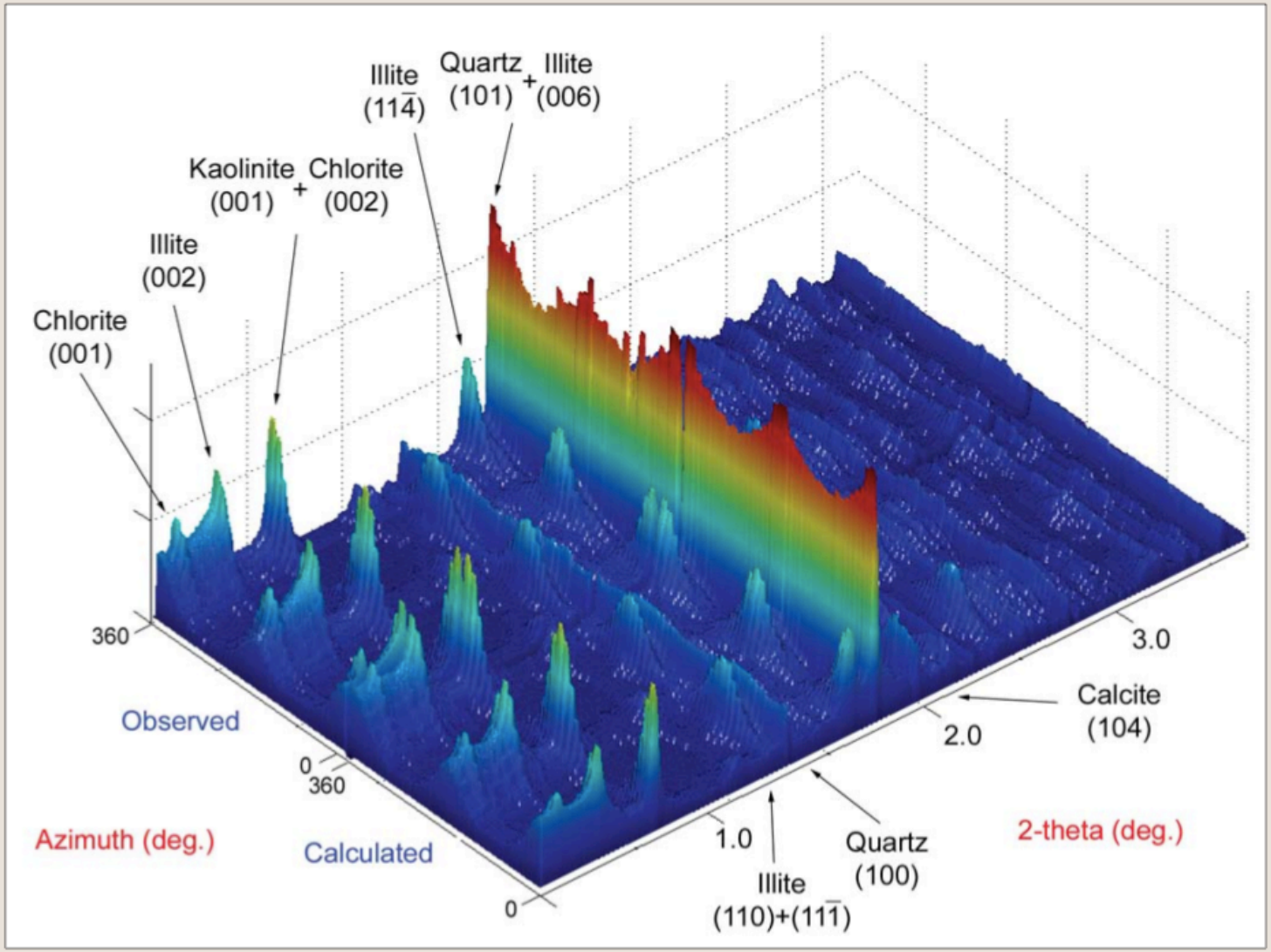

Figure 3. *3D representation of an "unrolled" image such as in Figure 2 (same color pattern is used). Some diffraction peaks are identified. The image compares observed intensities with calculated intensities based on the Rietveld refinements.*

Multi-phase

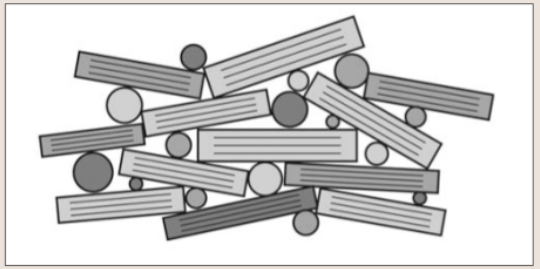

Figure 10. Sketch of a shale microstructure with intermixed platy and isometric crystals, porosity, and discrete grain contacts.

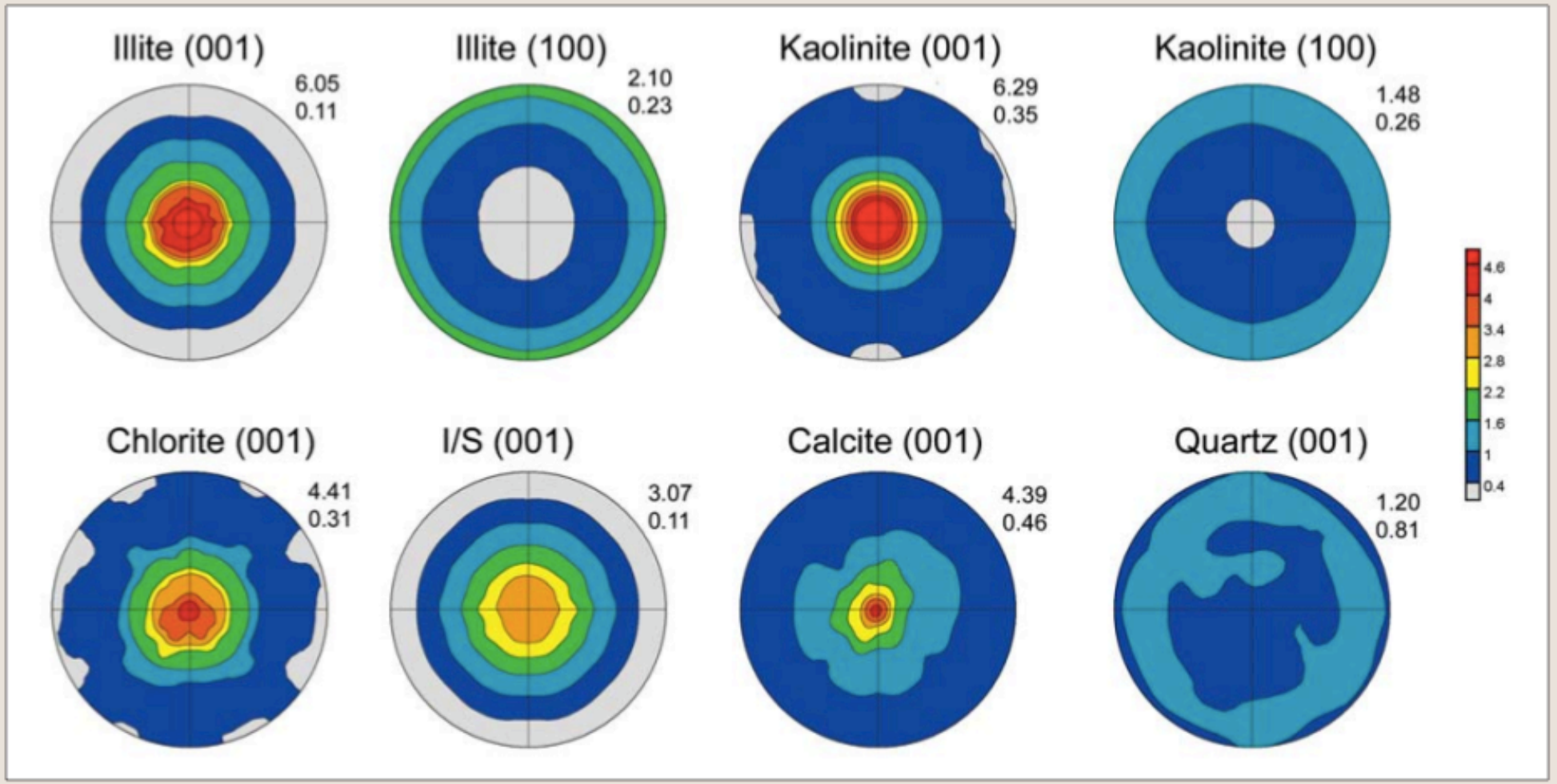

Figure 5. *Pole figures of illite, kaolinite, chlorite, illite/smectite, calcite, and quartz. Equal area projection. Pole densities are expressed in multiples of a random distribution (mrd). The numbers on the top right of each projection are maximum and minimum pole densities (in mrd).*

2D plate -> composition -> CPO

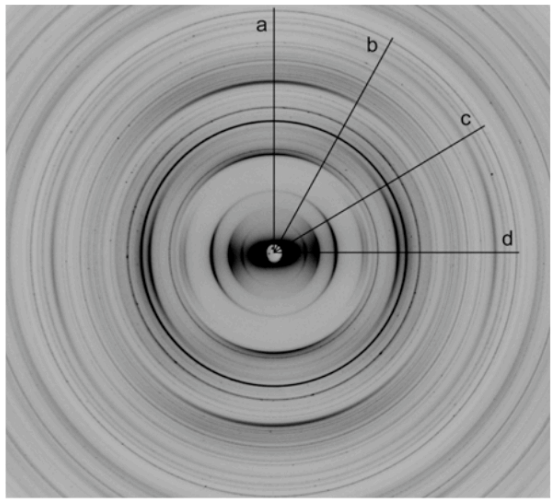

Figure 5. Diffraction image showing the strong preferred orientation of clay minerals in sample Mont Terri 1. The lines indicate the positions used to obtain the spectra illustrated in Figure 8.

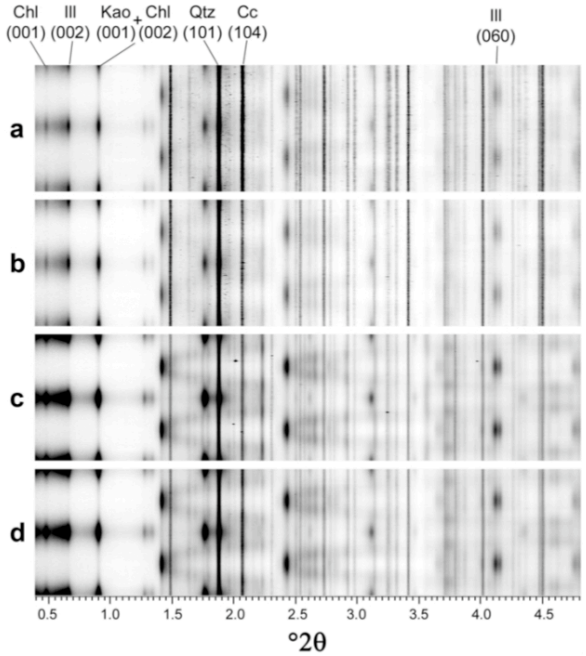

Figure 6. 2D plots of the four Benken samples with increasing depth as a function of diffraction image azimuth: the increase in texture strength is expressed in intensity variations. Some diffraction peaks are identified. A spotty pattern, *e.g.* for quartz and calcite, indicates larger grain size.

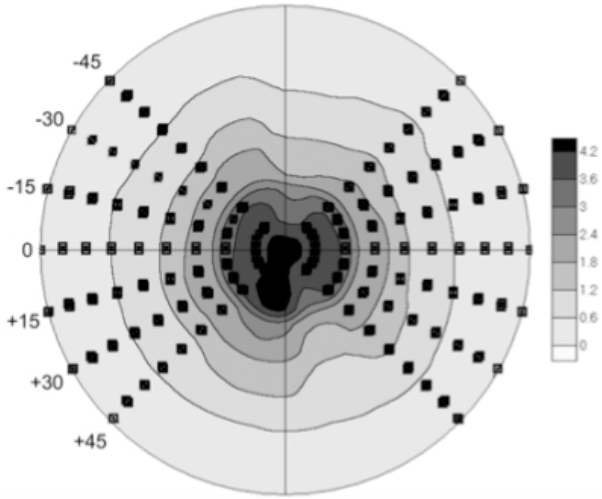

Figure 7. Pole figure coverage for the shale samples with seven measured images. The coverage pattern is superposed on a (001) illite pole figure. Equal area projection. The pole density contours are given in multiples of a random distribution (m.r.d.).

Orientation measurements: optical

- Principle: Refraction of light in optically anisotropic crystals
- Optical indicatrix (ellipsoid):

  cub: sphere → none

  hex, trig, tetra: uniaxial → c-axis direction

  ortho, mono, tricl: triaxial → indicatrix orientation
- Additional information from twin (cal) and/or cleavage planes (cpx)